

# Unitary Partitioning and the Contextual Subspace Variational Quantum Eigensolver

Alexis Ralli,<sup>1,\*</sup> Tim Weaving,<sup>1,†</sup> Andrew Tranter,<sup>2,3,‡</sup> William M. Kirby,<sup>2,§</sup> Peter J. Love,<sup>2,4,¶</sup> and Peter V. Coveney<sup>1,5,\*\*</sup>

<sup>1</sup>*Centre for Computational Science, Department of Chemistry, University College London, WC1H 0AJ, United Kingdom*

<sup>2</sup>*Department of Physics and Astronomy, Tufts University, Medford, MA 02155, USA*

<sup>3</sup>*Cambridge Quantum Computing, 9a Bridge Street Cambridge, CB2 1UB, United Kingdom*

<sup>4</sup>*Computational Science Initiative, Brookhaven National Laboratory, Upton, NY 11973, USA*

<sup>5</sup>*Informatics Institute, University of Amsterdam, Amsterdam, 1098 XH, Netherlands*

(Dated: August 16, 2022)

The contextual subspace variational quantum eigensolver (CS-VQE) is a hybrid quantum-classical algorithm that approximates the ground state energy of a given qubit Hamiltonian. It achieves this by separating the Hamiltonian into contextual and noncontextual parts. The ground state energy is approximated by classically solving the noncontextual problem, followed by solving the contextual problem using VQE, constrained by the noncontextual solution. In general, computation of the contextual correction needs fewer qubits and measurements compared to solving the full Hamiltonian via traditional VQE. We simulate CS-VQE on different tapered molecular Hamiltonians and apply the unitary partitioning measurement reduction strategy to further reduce the number of measurements required to obtain the contextual correction. Our results indicate that CS-VQE combined with measurement reduction is a promising approach to allow feasible eigenvalue computations on noisy intermediate-scale quantum devices. We also provide a modification to the CS-VQE algorithm, that previously could cause an exponential increase in Hamiltonian terms, that now at worst will scale quadratically.

## I. INTRODUCTION

One of the fundamental goals of quantum chemistry is to solve the time-independent non-relativistic Schrödinger Equation. The eigenvalues and eigenvectors obtained allow different molecular properties to be studied from first-principles. Standard methods project the problem onto a Fock space -  $\eta$  electrons distributed in  $M$  orbitals - and solve. Under this approximation, the number of possible determinants (configurations) scales factorially as  $\binom{M}{\eta}$  making the problem classically intractable for large  $M$  or  $\eta$  [1]. Quantum computers can efficiently represent the full configuration interaction (FCI) Hilbert space and offer a potential way to efficiently solve such molecular problems [2, 3]. This use case is often the canonical example of where the first quantum computers will be advantageous over conventional computers [4, 5].

In the fault-tolerant regime, quantum phase estimation (QPE) [6] provides a practical way to perform quantum chemistry simulations in polynomial time [2]. However, current noisy intermediate-scale quantum (NISQ) devices cannot implement this algorithm due to deep quantum circuits and long coherence times required [7, 8].

The constraints on present-day devices have given rise

to a family of quantum-classical algorithms that leverage as much classical processing as possible to reduce the quantum resources required to solve the problem at hand. Common examples of NISQ algorithms are the variational quantum eigensolver (VQE) [9], Quantum Approximate Optimization Algorithm (QAOA) [10] and Variational Quantum Linear Solver (VQLS) [11]. A good example is the recently proposed entanglement forging method [12], where the electronic structure problem for  $\text{H}_2\text{O}$  was reduced from 10 to multiple 5 qubits problems that were each studied using conventional VQE and classically combined. Recently another novel approach known as Quantum-Classical hybrid Quantum Monte Carlo (QC-QMC) was used to unbiased the sign problem in projector Monte Carlo (PMC) - which implements imaginary time evolution [13]. At a high level, the accuracy of a constrained PMC calculation is determined by the quality of trial wavefunctions. Quantum computers offer a way to efficiently store highly entangled trial wavefunctions and measure certain overlaps, that would require exponential resources classically. Huggins *et al.* performed QC-QMC simulations of different chemical systems on Google's Sycamore processor and obtain results competitive with state-of-the-art classical methods [13].

The contextual-subspace VQE algorithm is another hybrid quantum-classical approach [14]. It gives an approximate simulation method, where the quantum resources required can be varied for a trade off in accuracy. This allows problems to be studied where the full Hamiltonian would normally be too large to investigate on current NISQ hardware. This was shown in the original CS-VQE paper, where chemical accuracy for various molec-

\* alexis.ralli.18@ucl.ac.uk

† timothy.weaving.20@ucl.ac.uk

‡ tufts@atranter.net

§ william.kirby@tufts.edu

¶ peter.love@tufts.edu

\*\* p.v.coveney@ucl.ac.uk

ular systems was reached using significantly fewer qubits compared to that required for VQE on the full system [14]. As CS-VQE reduces the number of qubits required for simulation, the number of terms in a Hamiltonian requiring separate measurements is also reduced.

A natural question that arises from this is if this can be further reduced by measurement reduction schemes [15–28]. The goal of this work was to investigate the possible reductions given by the unitary partitioning strategy [15, 29, 30] and whether chemical accuracy on larger molecules can be reached on currently available NISQ hardware.

This paper is structured as follows. Section II summarises the CS-VQE algorithm. Here we provide a modification to the unitary partitioning step of the CS-VQE algorithm that previously could cause the number of terms in a Hamiltonian to exponentially increase, but now will at worst cause a quadratic increase. Section III is split into two main parts III B and III C. Section III B examines a model problem to exemplify each step of the CS-VQE algorithm. Section III C gives numerical results of applying unitary partitioning measurement reduction to a test bed of different molecular structure Hamiltonians, where the contextual subspace approximation has been employed.

## II. BACKGROUND

To keep our discussion self-contained and establish notation, we summarise the necessary background theory of the Contextual-Subspace VQE algorithm in this Section.

### A. Contextuality

The foundation of quantum contextuality is the Bell-Kochen-Specker (BKS) theorem [31]. In lay terms, every measurement provides a classical probability distribution (via the spectral theorem) and a joint distribution can be built as a product over all possible measurements [32]. The BKS theorem proves that it is impossible to reproduce the probabilities of every possible measurement outcome for a quantum system as marginals of this joint probability distribution [33]. This is related to how quantum mechanics does not allow models that are locally causal in a classical sense [34]. Contextuality is a generalization of nonlocality [34, 35]. This means that quantum measurement cannot be understood as simply revealing a pre-existing value of some underlying hidden variable [36, 37]. Bell’s theorem also reaches a similar conclusion against hidden variables [38], but in a different way.

A good example of this phenomenon is the “Peres-Mermin square” [37, 39], where no state preparation is involved and only observables are considered. We include an example in Appendix A and remark on the relation to VQE. Colloquially, for a noncontextual problem it is possible to assign deterministic outcomes to observables

simultaneously without contradiction; however, for a contextual problem this is not possible [14].

The following Subsections set out the Contextual Subspace VQE algorithm and we provide an alternate way to construct  $U_{\mathcal{W}}$  (defined below) compared to the original work [14]. This modification addresses the exponential scaling part of the method. Further background on the full CS-VQE algorithm is given in Appendix B.

### B. Contextual-Subspace VQE

Given a Hamiltonian expressed as:

$$\begin{aligned} H_{\text{full}} &= \sum_a c_a P_a = \sum_a c_a \left( \bigotimes_{j=0}^{n-1} \sigma_j^{(a)} \right) \\ &= \sum_a c_a (\sigma_0^{(a)} \otimes \sigma_1^{(a)} \otimes \dots \otimes \sigma_{n-1}^{(a)}), \end{aligned} \quad (1)$$

where  $c_a$  are real coefficients. Each Pauli operator  $P_a$  is made up of an  $n$ -fold tensor product of single qubit Pauli matrices  $\sigma_j \in \{\mathcal{I}, X, Y, Z\}$ , where  $j$  indexes the qubit the operator acts on. The CS-VQE algorithm is based on separating such a Hamiltonian into a contextual and noncontextual part [14]:

$$H_{\text{full}} = H_{\text{con}} + H_{\text{noncon}}. \quad (2)$$

As it is possible to assign definite values to all terms in  $H_{\text{noncon}}$  without contradiction, a classical hidden variable model (or quasi-quantised model) can be used to represent this system [40].

In [41], such a model is constructed along with a classical algorithm to solve it. This was based on the work of Spekkens [42, 43]. Solving this model yields a noncontextual ground state.

Once that solution is obtained, the remaining contextual part of the problem is solved. Solutions to  $H_{\text{con}}$  must be consistent with the noncontextual ground state, which defines a subspace of allowed states [14]. By projecting the problem into this subspace the overall energy is given by:

$$\begin{aligned} E(\vec{\theta}; \vec{q}, \vec{r}) &= E_{\text{noncon}}(\vec{q}, \vec{r}) + E_{\text{con}}(\vec{\theta}; \vec{q}, \vec{r}) \\ &= E_{\text{noncon}}(\vec{q}, \vec{r}) + \\ &\quad \frac{\langle \psi_{\text{con}}(\vec{\theta}) | Q_{\mathcal{W}}^\dagger U_{\mathcal{W}}^\dagger H_{\text{con}} U_{\mathcal{W}} Q_{\mathcal{W}} | \psi_{\text{con}}(\vec{\theta}) \rangle}{\langle \psi_{\text{con}}(\vec{\theta}) | Q_{\mathcal{W}}^\dagger Q_{\mathcal{W}} | \psi_{\text{con}}(\vec{\theta}) \rangle} \\ &= \frac{\langle \psi_{\text{con}}(\vec{\theta}) | Q_{\mathcal{W}}^\dagger U_{\mathcal{W}}^\dagger H_{\text{full}} U_{\mathcal{W}} Q_{\mathcal{W}} | \psi_{\text{con}}(\vec{\theta}) \rangle}{\langle \psi_{\text{con}}(\vec{\theta}) | Q_{\mathcal{W}}^\dagger Q_{\mathcal{W}} | \psi_{\text{con}}(\vec{\theta}) \rangle}. \end{aligned} \quad (3)$$

We have written  $U_{\mathcal{W}}$  rather than  $U_{\mathcal{W}}(\vec{q}, \vec{r})$  to simplify our notation.

The vector  $(\vec{q}, \vec{r})$  should be thought of as parameters that define a particular noncontextual state - normally

this will be a parameterization for the noncontextual ground state [14, 41]. This vector has size at most  $2n + 1$  for Hamiltonian defined on  $n$  qubits [41]. From  $(\vec{q}, \vec{r})$ , we define a set of stabilizers  $\mathcal{W}$  which stabilize that particular noncontextual state [14]. The unitary  $U_{\mathcal{W}}$  maps each of these stabilizers to a distinct single-qubit Pauli matrix - details of this are covered in II E. By enforcing the eigenvalue of these single-qubit Pauli operators we define a subspace of allowed quantum states that are consistent with the noncontextual state. To constrain the problem to this subspace, we use the projector  $Q_{\mathcal{W}}$ . Note this is not a unitary operation, hence the renormalization in equation 3. By projecting our contextual Hamiltonian into this subspace  $H_{\text{con}} \mapsto H_{\text{con}}^{\mathcal{W}} = Q_{\mathcal{W}}^{\dagger} U_{\mathcal{W}}^{\dagger} H_{\text{con}} U_{\mathcal{W}} Q_{\mathcal{W}}$ , we ensure solutions to  $H_{\text{con}}^{\mathcal{W}}$  remain in the subspace consistent with the noncontextual solution [14]. In other words, this operation means that solutions to  $H_{\text{con}}^{\mathcal{W}}$  will remain consistent with the noncontextual solution. Section II E goes into detail on this.

The contextual trial or Ansatz state is prepared as  $|\psi_{\text{con}}(\vec{\theta})\rangle = Q_{\mathcal{W}} U_{\mathcal{W}}^{\dagger} V(\vec{\theta}) |0\rangle^{\otimes n}$ , where  $V(\vec{\theta})$  is the parameterised operator that prepares it. The projector  $Q_{\mathcal{W}}$  restricts the action of  $V(\vec{\theta})$  to act on only the subspace of possible states consistent with the noncontextual ground state. Again this depends on which stabilizer eigenvalues are fixed. Again, as  $Q_{\mathcal{W}}$  is not a unitary operation the state must be re-normalized as:

$$|\psi_{\text{con}}(\vec{\theta})\rangle = \frac{Q_{\mathcal{W}} U_{\mathcal{W}}^{\dagger} V(\vec{\theta}) |0\rangle^{\otimes n}}{\sqrt{\langle 0|^{\otimes n} V^{\dagger}(\vec{\theta}) U_{\mathcal{W}} Q_{\mathcal{W}} Q_{\mathcal{W}} U_{\mathcal{W}}^{\dagger} V(\vec{\theta}) |0\rangle^{\otimes n}}} \quad (4)$$

Further analysis on the Contextual Subspace VQE projection ansatz is covered in [44]. In subsection II C we discuss how to solve the noncontextual problem.

### C. Noncontextual Hamiltonian

For a given noncontextual Hamiltonian, we define  $\mathcal{S}^{H_{\text{noncon}}}$  to be the set of  $P_i$  present in  $H_{\text{noncon}}$ . This set can be expanded as two subsets denoted as  $\mathcal{Z}$  and  $\mathcal{T}$ , representing the set of fully commuting operators and its complement respectively [14, 41]. The set  $\mathcal{T}$  can be expanded into  $N$  cliques, where operators within a clique must all commute with each other and operators between cliques pairwise anticommute. This is because commutation forms an equivalence relation on  $\mathcal{T}$  if and only if  $\mathcal{S}^{H_{\text{noncon}}}$  is noncontextual [14, 41].

A hidden variable model for such a system can be built, where the set of observables  $\mathcal{R}$  that define the phase-space points of the hidden variable model is [14, 41, 45]:

$$\begin{aligned} \mathcal{R} &\equiv \{P_0^{(j)} | j = 0, 1, \dots, N-1\} \cup \{G_0, G_1, G_2, \dots\} \\ &\equiv \{P_0^{(j)} | j = 0, 1, \dots, N-1\} \cup \mathcal{G}. \end{aligned} \quad (5)$$

The set  $\mathcal{G}$  represents an independent set of Pauli operators that generates the set of commuting observables  $\mathcal{Z}$ . Each  $P_0^{(j)}$  corresponds to a chosen Pauli operator in the  $j$ -th clique of  $\mathcal{T}$  - by convention we say this is the first operator in the set, but this can be any operator in the  $j$ -th clique.

With respect to the phase-space model given in [41], a valid noncontextual state is defined by the parameters  $(\vec{q}, \vec{r})$ , which set the expectation value of the operators in  $\mathcal{R}$  (Equation 5). Each operator in  $\mathcal{G}$  is assigned the value  $\langle G_i \rangle = q_i = \pm 1$ . The operators in  $\mathcal{T}$  are assigned the values  $\langle P_0^{(j)} \rangle = r_j$ , where  $\vec{r}$  is a unit vector ( $|\vec{r}| = 1$ ) [14, 41]. The number of elements in  $\vec{q}$  and  $\vec{r}$  are  $|\mathcal{G}|$  and  $N$  respectively. For  $n$  qubits the size of  $|\mathcal{R}|$  is bounded by  $2n + 1$ , which bounds the size of  $(\vec{q}, \vec{r})$  [41, 45].

The observables for the  $N$  anticommuting  $P_0^{(j)}$  operators in  $\mathcal{R}$  can be combined into the observable [41]:

$$A(\vec{r}) = \sum_{j=0}^{N-1} r_j P_0^{(j)}. \quad (6)$$

We denote the set of Pauli operators making up this operator as  $\mathcal{A} \equiv \{P_0^{(j)} | j = 0, 1, \dots, N-1\}$ .

The expectation value of  $A(\vec{r})$  is assigned by the hidden variable model to always be  $+1$ , due to:

$$\langle A(\vec{r}) \rangle = \sum_{j=0}^{N-1} r_j \langle P_0^{(j)} \rangle = \sum_{j=0}^{N-1} r_j r_j = \sum_{j=0}^{N-1} |r_j|^2 = +1, \quad (7)$$

using  $\langle P_0^{(j)} \rangle = r_j$  and  $|\vec{r}| = 1$ .

The expectation value for  $H_{\text{noncon}}$  can be induced, by setting the expectation values of operators in  $\mathcal{R}$  (Equation 5), as this set generates  $\mathcal{S}^{H_{\text{noncon}}}$  [14, 41]. To find the ground state of  $H_{\text{noncon}}$ , we perform a brute force search over this space. For each possible  $\pm 1$  combination of expectation values for each  $G_j$  ( $2^{|\mathcal{G}|}$  possibilities), the energy is minimized with respect to the unit vector  $\vec{r}$  - that sets the expectation values  $\langle P_0^{(j)} \rangle = r_j$ . Appendix B 1 d gives further algorithmic details. The vector  $(q, r)$  that was found to give the lowest energy defines the noncontextual ground state. Each noncontextual state  $(q, r)$ , corresponds to subspaces of quantum states, which we will describe in subsection II D.

### D. Contextual subspace

In [15] and [29] it was shown that an operator constructed as a normalised linear combination of pairwise anticommuting Pauli operators, like  $A(\vec{r})$  (Equation 6), is equivalent to a single Pauli operator up to a unitary rotation  $R$ . We can therefore write  $A(\vec{r}) \mapsto P_0^{(k)} = R A(\vec{r}) R^{\dagger}$  for a selected  $P_0^{(k)} \in \mathcal{A}$ . We write the set  $\mathcal{R}_{\vec{r}}$  (Equation 5) under this transformation:

$$\mathcal{R}_{\vec{r}} \equiv \{A(\vec{r})\} \cup \mathcal{G} \mapsto \mathcal{R}' \equiv \underbrace{\{P_0^{(k)}\}}_{P_0^{(k)} = RA(\vec{r})R^\dagger} \cup \mathcal{G}. \quad (8)$$

It will be shown later that the unitary  $R$  is constructed from the operators in  $\mathcal{A}$ . This means the terms in  $\mathcal{G}$  are unaffected by this transformation, as operators in  $\mathcal{G}$  must universally commute so must commute with  $R$ .

A given noncontextual state  $(\vec{q}, \vec{r})$  is equivalent to the joint expectation value assignment of  $\langle G_i \rangle = q_i = \pm 1$  and  $\langle A(\vec{r}) \rangle = +1$ . This defines a set of stabilizers:

$$\mathcal{W}_{all} \equiv \{q_0 G_0, q_1 G_1, \dots, q_{|\mathcal{G}|-1} G_{|\mathcal{G}|-1}, A(\vec{r})\}, \quad (9)$$

which by definition must stabilize that noncontextual state  $(\vec{q}, \vec{r})$  or more precisely, the subspace of quantum states corresponding to it<sup>1</sup>. Note  $A(\vec{r})$  is not a conventional stabilizer, but is unitarily equivalent to a single qubit operator  $P_0^{(k)}$  [15, 29].

We can consider this problem under the unitary transform defined in Equation 8. The stabilizers in  $\mathcal{W}_{all}$  become:

$$\mathcal{W}'_{all} \equiv \{q_0 G_0, q_1 G_1, \dots, q_{|\mathcal{G}|-1} G_{|\mathcal{G}|-1}, \xi P_0^{(k)}\}, \quad (10)$$

which defines a regular set of stabilizers for the noncontextual state  $(\vec{q}, \vec{r})$ , which defines a subspace of quantum states. Here  $\xi = \pm 1$  and is determined by  $RA(\vec{r})R^\dagger = \xi P_0^{(k)}$  and can always be chosen to be +1, which we do throughout this paper.

Altogether, when certain noncontextual stabilizers are fixed (by the noncontextual state) they specify a subspace of allowed quantum states that will be consistent with that noncontextual state and thus define the constraints for the contextual part of the problem. We refer to this subspace as the contextual subspace [14].

### E. Mapping a contextual subspace to a stabilizer subspace

In CS-VQE, the expectation value of the full Hamiltonian is obtained according to Equation 3. First, the noncontextual problem is solved yielding the noncontextual state  $(\vec{q}, \vec{r})$  - normally the ground state  $(\vec{q}_0, \vec{r}_0)$ . Appendix B 1 d shows how  $(\vec{q}_0, \vec{r}_0)$  can be obtained via a brute force approach. Next the contextual Hamiltonian is projected into the subspace of allowed quantum states consistent with the defined noncontextual state. This constraint is imposed via:  $H_{full} \mapsto H'_{full} = Q_{\mathcal{W}}^\dagger U_{\mathcal{W}}^\dagger H_{full} U_{\mathcal{W}} Q_{\mathcal{W}}$ , where the expectation value is then found on a quantum device.

The unitary operation  $U_{\mathcal{W}}$  is defined by the set of contextual stabilizers  $\mathcal{W} \subseteq \mathcal{W}_{all}$  (equation 9) that eigenvalue we fix according to the noncontextual state. If  $A(\vec{r}) \in \mathcal{W}$ , meaning  $\langle A(\vec{r}) \rangle$  is fixed to be +1, then the steps summarised in Equation 8 must first be performed to reduce  $A(\vec{r})$  to a single Pauli operator. Clifford operators  $V_i(P)$  are then used to map each  $P \in \mathcal{W}$  to a single-qubit  $Z$  operator. Each  $V_i$  is made up of at most two  $\frac{\pi}{2}$ -rotations per element in  $\mathcal{W}$ . In [14] it was shown that at most there will be  $2n$  Clifford rotations required for  $n$  qubits [46]. We can write this operator as:

$$U_{\mathcal{W}}^\dagger(\vec{q}, \vec{r}) = \begin{cases} \prod_{P_i \in \mathcal{W} \subseteq \mathcal{W}_{all}} V_i(P_i), & \text{if } A(\vec{r}) \notin \mathcal{W} \\ \left( \prod_{P_i \in \mathcal{W} \subseteq \mathcal{W}_{all}} V_i(P_i) \right) R, & \text{if } A(\vec{r}) \in \mathcal{W} \end{cases} \quad (11)$$

Applying  $U_{\mathcal{W}}^\dagger \mathcal{W} U_{\mathcal{W}} = \mathcal{W}^Z$  results in a set of single-qubit  $Z$  Pauli operators. An implementation note is that each operator  $V_i(P_i)$  in  $U_{\mathcal{W}}$  depends on each other - this can be seen by expanding  $U_{\mathcal{W}}^\dagger \mathcal{W} U_{\mathcal{W}}$ . Therefore, each  $V_i$  operator is dependent on the stabilizers in  $\mathcal{W}$  and in what order they occur. We recursively define each  $V_i$  as follows:

1. Set  $\mathcal{W} = R\mathcal{W}R^\dagger$  iff  $A(\vec{r}) \in \mathcal{W}$ .
2. Find the unitary  $V_0$  mapping the first Pauli operator  $P_0 \in \mathcal{W}$  to a single qubit Pauli operator.
3. Apply this operator to each operator in the set:  $V_0 \mathcal{W} V_0^\dagger = \mathcal{W}^{(0)}$ .
4. Find the unitary  $V_1$  mapping  $V_0 P_1 V_0^\dagger \in \mathcal{W}^{(0)}$  to a single-qubit  $Z$  Pauli operator.
5. Apply this operator to all operators in the set:  $V_1 \mathcal{W}^{(0)} V_1^\dagger = \mathcal{W}^{(1)}$ .
6. Repeat this procedure from step (3) until all the operators are mapped to single qubit  $Z$  Pauli operators:  $\mathcal{W} \mapsto \mathcal{W}^Z$ .

Finally, the eigenvalue of the single-qubit  $Z$  Pauli stabilizers in  $\mathcal{W}^Z$  are defined by the vector  $\vec{q}$  of the noncontextual ground state  $(\vec{q}, \vec{r})$ , note  $\langle A(\vec{r}) \rangle$  is fixed to +1 and thus  $\vec{r}$  isn't important here.  $U_{\mathcal{W}}$  can flip the sign of these assignments, but it is efficient to classically determine by tracking how  $U_{\mathcal{W}}$  affects the sign of the operators in  $\mathcal{W}$ .

To project the Hamiltonian into the subspace consistent with the noncontextual state, we first perform the following rotation  $H_{full} \mapsto H_{full}^{\mathcal{W}} = U_{\mathcal{W}}^\dagger H_{full} U_{\mathcal{W}}$ . As this is a unitary transform, the resultant operator has the same spectrum as before. We then restrict the rotated Hamiltonian to the correct subspace by enforcing the eigenvalue of the operators in  $\mathcal{W}^Z$  - where the outcomes are defined by the noncontextual state. As each operator in  $\mathcal{W}^Z$  only acts nontrivially on a unique qubit, each stabilizer fixes the state of that qubit to be either  $|0\rangle$  or  $|1\rangle$ . We write this state as:

<sup>1</sup> Note a stabilizer for a state leaves it unchanged. For example if  $O$  stabilizes  $|\psi\rangle$  then  $O|\psi\rangle = |\psi\rangle$

$$|\psi_{\text{fixed}}\rangle = \bigotimes_{P_v \in \mathcal{W}^Z} |i\rangle_v \begin{cases} i = 0, & \text{if } \langle P_v \rangle = +1 \\ i = 1, & \text{if } \langle P_v \rangle = -1 \end{cases}, \quad (12)$$

where  $v$  indexes the qubit a given single-qubit stabilizer acts on and  $\langle P_v \rangle$  is defined by the noncontextual state. We can write the projector onto this state as:

$$Q_{\mathcal{W}} = |\psi_{\text{fixed}}\rangle \langle \psi_{\text{fixed}}| \otimes \mathcal{I}_{(n-|\mathcal{W}^Z|)} \quad (13)$$

where  $\mathcal{I}_{(n-|\mathcal{W}^Z|)}$  is the identity operator acting on the  $(n-|\mathcal{W}^Z|)$  qubits not fixed by the single-qubit  $P_v$  stabilizers. The action on a general state  $|\phi\rangle$  is:

$$Q_{\mathcal{W}} |\phi\rangle = |\psi_{\text{fixed}}\rangle \langle \psi_{\text{fixed}}| \phi\rangle \otimes |\phi\rangle_{(n-|\mathcal{W}^Z|)} \quad (14)$$

where  $Q_{\mathcal{W}}$  has only fixed the state of qubits  $v$  and thus each stabilizer  $P_v$  removes a one qubit from the problem. As the states of these qubits are fixed, the expectation value of the single-qubit Pauli matrices indexed on qubits  $v$  are known. Thus the Pauli operators in the rotated Hamiltonian  $H_{\text{full}}^{\mathcal{W}} = U_{\mathcal{W}}^\dagger H_{\text{full}} U_{\mathcal{W}}$  acting on these qubits can be updated accordingly and the Pauli matrices on qubits  $v$  dropped. Any term in the rotated Hamiltonian that anticommutes with a fixed generator  $P_v$  is forced to have an expectation value of zero and can be completely removed from the problem Hamiltonian. The resultant Hamiltonian acts on  $|\mathcal{W}^Z|$  fewer qubits. We denote this operation as  $H_{\text{full}} \mapsto H_{\text{full}}^{\mathcal{W}'} = Q_{\mathcal{W}}^\dagger U_{\mathcal{W}}^\dagger H_{\text{full}} U_{\mathcal{W}} Q_{\mathcal{W}}$ . The noncontextual approximation will be stored in the identity term of the problem and therefore doesn't need to be tracked separately.

The choice of which stabilizer eigenvalues to fix (i.e. what is included in  $\mathcal{W}$ ) and which to allow to vary remains an open question of the CS-VQE algorithm. In this work, we use the heuristic given in [14] that begins at the full noncontextual approximation, where  $\mathcal{W}$  contains all possible stabilizers. We then add a qubit to the quantum correction, by removing an operator from  $\mathcal{W}$  and greedily choosing each pair that gives the lowest ground state energy estimate [14]. Alternative strategies on how to do this remain an open question of CS-VQE. A possible way to approach this problem is to look at the priority of different terms in  $H_{\text{con}}$  [47]. Note that the quality of the approximation is sensitive to which stabilizers are included in  $\mathcal{W}$ . When fewer stabilizers are considered (included in  $\mathcal{W}$ ), the resultant rotated Hamiltonians will act on more qubits and approximate the true ground state energy better.

In [14], Kirby *et al.* construct  $R$  as a sequence of rotations (exponentiated Pauli operators) defined by  $A(\vec{r})$  as in the unitary partitioning method [15, 29]. We denote this operation  $R_S$ . Appendix B 2 a gives the full definition of this operator. If  $R_S$  is considered as just an arbitrary sequence of exponentiated Pauli operator rotations, then the transformation  $H_{\text{full}} \mapsto H_{\text{full}}^{R_S} = R_S H_{\text{full}} R_S^\dagger$  results in an operator whose terms have increased by a

factor of  $\mathcal{O}(2^N)$ , where  $N$  is the number of cliques defined from  $\mathcal{T}$  [14]. This presented a possible roadblock for the CS-VQE algorithm, as classically precomputing  $U_{\mathcal{W}}^\dagger H_{\text{full}} U_{\mathcal{W}}$  could cause the number of terms to exponentially increase. We give a further analysis of this in Appendix B 2 a. Additional structure between  $R_S$  and  $H_{\text{full}}$  can make the base of the exponent slightly lower; however, the scaling still remains exponential in the number of qubits  $n$ , where  $|\mathcal{A}| \leq 2n + 1$  [41]. The only case in which there is not an exponential increase in terms is for the trivial instance that  $R_S$  commutes with  $H_{\text{full}}$ . In the next section, we provide an alternative construction of  $R$  via a linear combination of unitaries that results in only a quadratic increase in the number of terms of the Hamiltonian when transformed. This avoids the need to apply the unitary partitioning operator  $R$  (via a sequence of rotations) coherently in the quantum circuit after the ansatz circuit, which was the proposed in [14].

## F. Linear combination of unitaries construction of $R$

In the unitary partitioning method [15, 29], it was shown that  $R$  could also be built as a linear combination of Pauli operators [15, 30]. We provide the full construction in Appendix B 2 b and denote the operator as  $R_{LCU}$ . Rotating a general Hamiltonian  $H_{\text{full}}$  by this operation  $R_{LCU}$  results in:

$$\begin{aligned} R_{LCU} H_{\text{full}} R_{LCU}^\dagger &= \sum_i^{|H_{\text{full}}|} (\mu_i) P_i + \\ &\sum_j^{|\mathcal{A}|-1} \sum_{\substack{i \\ \forall \{P_j, P_k, P_i\}=0}}^{|H_{\text{full}}|} \mu_{ij} P_j P_k P_i + \\ &\sum_j^{|\mathcal{A}|-1} \sum_i^{|H_{\text{full}}|} \sum_{\substack{l > j \\ \forall \{P_i, P_j, P_l\}=0}}^{|\mathcal{A}|-1} \mu_{ijl} P_i P_j P_l. \end{aligned} \quad (15)$$

The Pauli operators  $P_j$ ,  $P_k$  and  $P_l$  are operators in  $\mathcal{A}$ , further details are covered in Appendix B 2 b. Overall, this unitary transformation causes the number of terms in the Hamiltonian to scale as  $\mathcal{O}(|H_{\text{full}}| \cdot |\mathcal{A}|^2)$ . This scaling is quadratic in the size of  $\mathcal{A}$  and as  $|\mathcal{A}| \leq 2n + 1$  [41], the number of terms in the rotated system will at worst scale quadratically with the number of qubits  $n$ . Unlike the sequence of rotations approach, this non-Clifford operation doesn't cause the number of terms in a Hamiltonian to increase exponentially.

The transformation given in Equation 15  $H_{\text{full}} \mapsto H_{\text{full}}^{LCU'} = R_{LCU}^\dagger H_{\text{full}} R_{LCU}$  is performed classically in CS-VQE. This is efficient to do because it just involves Pauli operator multiplication, which can be done symbolically or via a symplectic approach [48]. This operation could be applied within the quantum circuit. However, con-

trary to the deterministic sequence of rotations approach, this implementation would be probabilistic as it requires post selection on an ancillary register [15, 30, 49, 50]. Amplitude amplification techniques could improve this, but would require further coherent resources [51–54]. Doing this transformation in a classical preprocessing step therefore reduces the coherent resources required and at worst increases the number of terms needing measuring quadratically with respect to the number of qubits.

### G. CS-VQE Implementation

In [14],  $U_{\mathcal{W}}(\vec{q}, \vec{r})$  was fixed to include all the stabilizers of the noncontextual ground state  $\mathcal{W} \equiv \mathcal{W}_{all}$  (Equation 9), rather than possible subsets  $\mathcal{W} \subseteq \mathcal{W}_{all}$ . The whole Hamiltonian was mapped according to  $H_{full} \mapsto H_{full}^{\mathcal{W}_{all}} = U_{\mathcal{W}_{all}}^\dagger H_{full} U_{\mathcal{W}_{all}}$ . In general  $A(\vec{r}) \in \mathcal{W}$  and  $U_{\mathcal{W}_{all}}$  will therefore normally include the unitary partitioning operator  $R$ . The problem with this approach is the unitary  $R$  is not a Clifford operation and the transformation can cause the number of terms in the Hamiltonian to increase. This increase is exponential if  $R_S$  is used and quadratic if  $R_{LCU}$  is employed. As this step can generate more terms,  $R$  should only be included in  $U_{\mathcal{W}}$  if the eigenvalue of  $A(\vec{r})$  is fixed to +1, otherwise it is a redundant operation as the spectrum of the operator rotated by  $R$  is unchanged. We therefore modify the CS-VQE algorithm to construct  $U_{\mathcal{W}}$  from the CS-VQE noncontextual generator eigenvalues that are fixed. This means  $\mathcal{W} \subseteq \mathcal{W}_{all}$  and ensures that the number of terms can only increase if the eigenvalue of  $A(\vec{r})$  is fixed.

## III. NUMERICAL RESULTS

We split our results into two subsections. First, we explore a toy problem, showing the steps of the CS-VQE algorithm. We show how classically applying  $R$  without fixing the eigenvalue of  $A(\vec{r})$  to +1 can unnecessarily increase the number of terms in a Hamiltonian without changing its spectrum. Finally, in Section III C we apply measurement reduction combined with CS-VQE to a set of electronic structure Hamiltonians and show that this can significantly reduce the number of terms requiring separate measurement. The raw data for these results is supplied in ancillary files hosted on arXiv.

### A. Method

We investigated the same electronic structure Hamiltonians considered in the original CS-VQE paper [14]. All molecules considered had a multiplicity of 1 and thus a singlet ground state. The same qubit tapering was performed to remove the  $\mathbb{Z}_2$  symmetries [55]. For each tapered Hamiltonian, we generate a set of reduced Hamiltonians  $\{Q_{\mathcal{W}}^\dagger U_{\mathcal{W}}^\dagger H_{full} U_{\mathcal{W}} Q_{\mathcal{W}}\}$  where the size of  $\mathcal{W}$  varies

from 1 to  $|\mathcal{W}_{all}|$ , representing differing noncontextual approximations, as summarised in Section II G. To generate the different CS-VQE Hamiltonians, we modify the original CS-VQE source code used in [14, 56]. The code was modified to implement the unitary partitioning step of CS-VQE if and only if the eigenvalue of  $A(\vec{r})$  was fixed. This ensured the number of terms in the rotated Hamiltonian didn't increase unnecessarily, as described in Section II G.

For each electronic structure Hamiltonian generated in this way, we then apply the unitary partitioning measurement reduction scheme to further reduce the number of terms requiring separate measurement [15, 29, 30]. Partitioning into anticommuting sets was performed using NETWORKX [57]. A graph of the qubit Hamiltonian is built, where nodes represent Pauli operators and edges are between nodes that commute. A graph coloring can be used to find the anticommuting cliques of the graph. This searches for the minimum number of colors required to color the graph, where no neighbors of a node can have the same color as the node itself. The ‘‘largest first’’ coloring strategy in NETWORKX was used in all cases [57, 58].

We calculate the ground state energy of each Hamiltonian in this study by directly evaluating the lowest eigenvalues. This was achieved by diagonalising them on a conventional computer.

### B. Toy Example

We consider the following qubit Hamiltonian:

$$\begin{aligned}
 H = & 0.6 I I Y I + 0.7 X Y X I + 0.7 X Z X I + 0.6 X Z Z I + \\
 & 0.1 Y X Y I + 0.7 Z Z Z I + 0.5 I I I Z + 0.1 X X X I + \\
 & 0.5 X X Y I + 0.2 X X Z I + 0.2 Y X X I + 0.2 Y Y Z I + \\
 & 0.1 Y Z X I + 0.1 Z Y Y I,
 \end{aligned} \tag{16}$$

and use it to exemplify the steps of the CS-VQE algorithm. The results are reported to 3 decimal places and full numerical details can be found in Appendix C.

Following the steps given in Appendix B 1 b, we first split the Hamiltonian into its contextual and noncontextual parts (Equation 2):

$$\begin{aligned}
 H_{\text{noncon}} = & 0.5 \underbrace{I I I Z}_{\mathcal{Z}} + \\
 & 0.7 X Z X I + 0.7 Z Z Z I + \\
 & 0.1 Y X Y I + 0.6 I I Y I + \\
 & \underbrace{0.7 X Y X I + 0.6 X Z Z I}_{\mathcal{T}}
 \end{aligned} \tag{17a}$$

$$\begin{aligned}
 H_{\text{con}} = & 0.1 X X X I + 0.5 X X Y I + 0.2 X X Z I + \\
 & 0.2 Y X X I + 0.2 Y Y Z I + 0.1 Y Z X I + \\
 & 0.1 Z Y Y I.
 \end{aligned} \tag{17b}$$

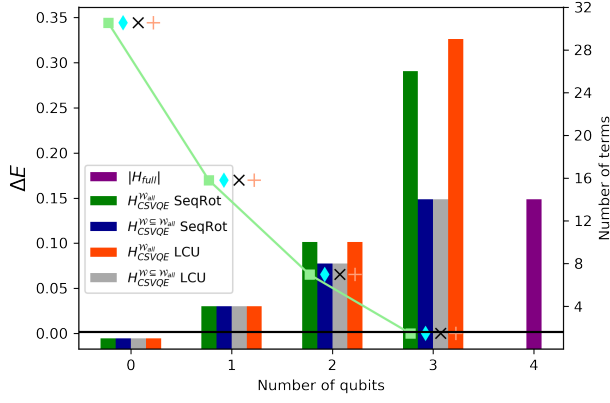


FIG. 1: Ground state energy and the number of terms of different contextual subspace projected Hamiltonians generated in CS-VQE. Each Hamiltonian has been transformed as  $Q_{\mathcal{W}}^\dagger U_{\mathcal{W}}^\dagger H U_{\mathcal{W}} Q_{\mathcal{W}}$ , apart from the four qubit case, which is the full  $H$ . The scatter plot is associated with left-hand y-axis and gives the energy error as:  $\Delta E = |E_{approx} - E_{true}|$ . The bar chart gives the number of terms in each Hamiltonian and is associated with the right-hand y-axis. From left to right the following generators are fixed:  $\{YIYI, IXYI, IIIZ, \mathcal{A}(\vec{r}_0)\}$ ,  $\{IXYI, IIIZ, \mathcal{A}(\vec{r}_0)\}$ ,  $\{IXYI, IIIZ, \}$ ,  $\{IIIZ\}$  and  $\{\}$ . The  $\mathcal{W} = \{\}$  case represents standard full VQE over the full problem. The 0 qubit case presents the scenario where the problem is fully noncontextual and no quantum correction is made. Tables IV and V in Appendix C give the details on how Hamiltonian is built. The horizontal black line indicates an error of  $1.6 \times 10^{-3}$ .

Each row after the first in Equation 17a, is a clique of  $\mathcal{T}$ . From here, we define the set  $\mathcal{R}$  (Equation 5):

$$\mathcal{R} = \underbrace{\{YIYI, IXYI, IIIZ\}}_{\mathcal{G}} \cup \underbrace{\{XZXI, YXYI, XYXI\}}_{\{P_0^{(j)} | j=0,1,\dots,N-1\}} \quad (18)$$

Note how different combinations of the operators in Equation 18, allow all the operators in  $H_{\text{noncon}}$  (Equation 17a) to be inferred under the Jordan product, defined as:  $P_a \circ P_b = \frac{\{P_a, P_b\}}{2}$ . Basically, the Jordan product is equal to the regular matrix product if the operators commute, and equal to zero if the operators anticommute. Next the noncontextual problem was solved.

The expectation value for  $H_{\text{noncon}}$  can be induced, by setting the expectation values of operators in  $\mathcal{R}$  (Equation 18), as the Pauli operators in  $H_{\text{noncon}}$  are generated by  $\mathcal{R}$  under the Jordan product. The expectation value of each operator in  $H_{\text{noncon}}$  can therefore be inferred without contradiction. To find the ground state of  $H_{\text{noncon}}$ , we checked all possible  $\pm 1$  expectation values for each  $G_j$  ( $2^3 = 8$  possibilities). For each possible  $\pm 1$  combination, the energy was minimized with respect to the unit vector  $\vec{r}$ , which sets the expectation value for each  $\langle P_0^{(j)} \rangle = r_j$ .

molecule	basis	# gates for $R_S$
BeH <sub>2</sub>	(STO-3G)	[90, 72]
Mg	(STO-3G)	[189, 162]
H <sub>3</sub> <sup>+</sup>	(3-21G)	[209, 176]
O <sub>2</sub>	(STO-3G)	[184, 160]
OH <sup>-</sup>	(STO-3G)	[104, 80]
CH <sub>4</sub>	(STO-3G)	[325, 286]
Be	(STO-3G)	[14, 8]
NH <sub>3</sub>	(STO-3G)	[299, 260]
H <sub>2</sub> S	(STO-3G)	[120, 96]
H <sub>2</sub>	(3-21G)	[66, 48]
HF	(3-21G)	[735, 672]
F <sub>2</sub>	(STO-3G)	[133, 112]
HCl	(STO-3G)	[36, 24]
HeH <sup>+</sup>	(3-21G)	[88, 64]
MgH <sub>2</sub>	(STO-3G)	[403, 364]
CO	(STO-3G)	[325, 286]
LiH	(STO-3G)	[36, 24]
N <sub>2</sub>	(STO-3G)	[207, 180]
NaH	(STO-3G)	[493, 442]
H <sub>2</sub> O	(STO-3G)	[120, 96]
H <sub>3</sub> <sup>+</sup>	(STO-3G)	[3, 0]
LiOH	(STO-3G)	[378, 336]
LiH	(3-21G)	[459, 408]
H <sub>2</sub>	(6-31G)	[66, 48]
NH <sub>4</sub> <sup>+</sup>	(STO-3G)	[325, 286]
HF	(STO-3G)	[36, 24]

TABLE I: Gate requirements to implement  $R$  as a sequence of rotations in the unitary partitioning measurement reduction step. The square tuple gives the upper bound on the number of single qubit and CNOT gates required - [*single*, *CNOT*]. These resource requirements are based on the largest anticommuting clique of each Hamiltonian, as these have the largest circuit requirements for  $R_S$ .

Appendix B1d gives further algorithmic details. The vector  $(\vec{q}, \vec{r})$  that was found to give the lowest energy defines the noncontextual ground state. In this case the ground state is:

$$\underbrace{(-1, +1, -1)}_{\vec{q}_0} \underbrace{(+0.253, -0.658, -0.709)}_{\vec{r}_0} \quad (19)$$

This noncontextual state defines the operator  $\mathcal{A}(\vec{r}_0)$ :

$$\mathcal{A}(\vec{r}_0) = 0.253 YXYI - 0.658 XYXI - 0.709 XZXI \quad (20)$$

From this we can write  $\mathcal{R}_{\vec{r}}$  (Equation 8)

$$\mathcal{R}_{\vec{r}} \equiv \{\mathcal{A}(\vec{r}_0)\} \cup \{YIYI, IXYI, IIIZ\} \quad (21)$$

To map  $\mathcal{A}(\vec{r}_0)$  to a single Pauli operator we use unitary partitioning [15, 29, 30]. The required unitary can be constructed as either a sequence of rotations [15]:

$$R_S = e^{-1i \cdot 0.788 \cdot ZYZI} \cdot e^{+1i \cdot 1.204 \cdot ZZZI} \quad (22)$$

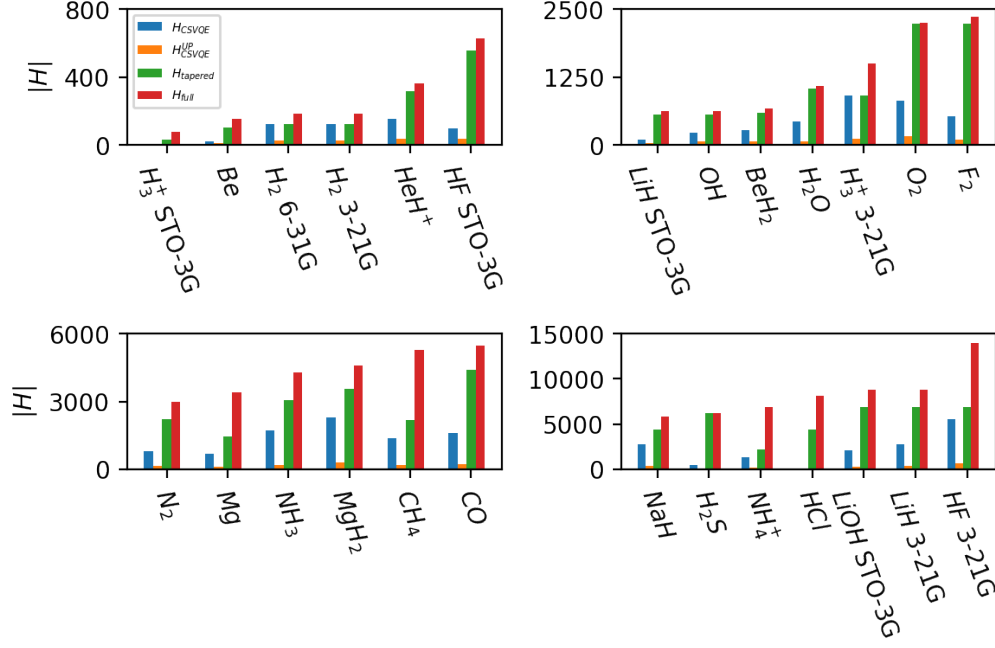


FIG. 2: Number of Pauli operators in different electronic structure Hamiltonians required to achieve chemical accuracy. For each molecule the full Hamiltonian, tapered Hamiltonian, CS-VQE and CS-VQE with unitary partitioning measurement reduction applied are given. Table VI in the Appendix gives numerical details of each. The size of the Hamiltonian for LiH (3-21G singlet) with measurement reduction applied is different for the sequence of rotations and LCU unitary partitioning methods. This is an artifact of the graph colour heuristic finding different anticommuting cliques in the CS-VQE Hamiltonian.

or linear combination of unitaries [15]:

$$R_{LCU} = 0.792IIII + 0.416iZZZI - 0.448iZYZI. \quad (23)$$

These operators perform the following reduction:  $R_S A(\vec{r}_0) R_S^\dagger = R_{LCU} A(\vec{r}_0) R_{LCU}^\dagger = YXYI$ .

If the eigenvalue of  $A(\vec{r}_0)$  is fixed, then we should consider  $\mathcal{R}_{\vec{r}}$  (Equation 21) under the unitary transform  $R_{LCU}$  or  $R_S$  (Equation 8):

$$\begin{aligned} \mathcal{R}' &= R_{S/LCU} A(\vec{r}) R_{S/LCU}^\dagger \cup \{YIYI, IXYI, IIIZ\} \\ &= \{YXYI\} \cup \{YIYI, IXYI, IIIZ\}. \end{aligned} \quad (24)$$

Equations 19, 21 and 24 define the noncontextual stabilizers:

$$\begin{aligned} \mathcal{W}_{all} &\equiv \{+1 A(\vec{r}_0), -1 YIYI, +1 IXYI, -1 IIIZ\}, \\ \mathcal{W}'_{all} &\equiv \{+1 YXYI, -1 YIYI, +1 IXYI, -1 IIIZ\}. \end{aligned} \quad (25)$$

Next, we define different  $U_{\mathcal{W}}$  (Equation 11), depending on which stabilizers  $\mathcal{W}$  we wish to fix. For this problem we found the optimal ordering of which stabilizers to fix, via brute force, to be  $\{-1 YIYI, +1 IXYI, +1 A(\vec{r}_0), -1 IIIZ\}$  followed by  $\{+1 IXYI, -1 IIIZ, +1 A(\vec{r}_0)\}$  followed by  $\{+1 IXYI, -1 IIIZ\}$  followed by  $\{-1 IIIZ\}$ .

This defines a set of four different  $\mathcal{W}$ , representing different noncontextual approximations. These give four different  $U_{\mathcal{W}}$  built according to Equation 11. Table IV in Appendix C gives the full definition of each operator.

Taking a specific example, for  $\mathcal{W} = \{+IXYI, -IIIZ, +A(\vec{r}_0)\}$  we define  $U_{\mathcal{W}}^\dagger$  (Equation 11). This operator transforms  $\mathcal{W}$  as  $\mathcal{W}^Z = U_{\mathcal{W}}^\dagger \mathcal{W} U_{\mathcal{W}} = \{+IZII, -IIIZ, +IIZI\}$ . The eigenvalues of the operators in  $\mathcal{W}^Z$  are fixed by the noncontextual state to be  $\langle IZII \rangle = +1$ ,  $\langle IIZI \rangle = +1$ ,  $\langle IIIZ \rangle = -1$ . This defines the projector:

$$\begin{aligned} Q_{\mathcal{W}} &= \left( \underbrace{|0\rangle\langle 0| + |1\rangle\langle 1|}_{\mathcal{I}_{(n-|\mathcal{W}^Z|)}} \right) \otimes \underbrace{|0\rangle\langle 0| \otimes |0\rangle\langle 0| \otimes |1\rangle\langle 1|}_{|\psi^{\text{fixed}}\rangle} \\ &= I \otimes |001\rangle\langle 001|. \end{aligned} \quad (26)$$

The reduced Hamiltonian is therefore:

$$\begin{aligned} H \mapsto H_{\mathcal{W}}^{LCU} &= Q_{\mathcal{W}}^\dagger U_{\mathcal{W}}^\dagger (LCU) H_{\text{full}} U_{\mathcal{W}} (LCU) Q_{\mathcal{W}} \\ &= -1.827 I - 0.414 X - 0.292 Z + 0.648 X. \end{aligned} \quad (27)$$

Appendix C gives further details on this operation and provides the specifics for the other projected Hamiltonians.

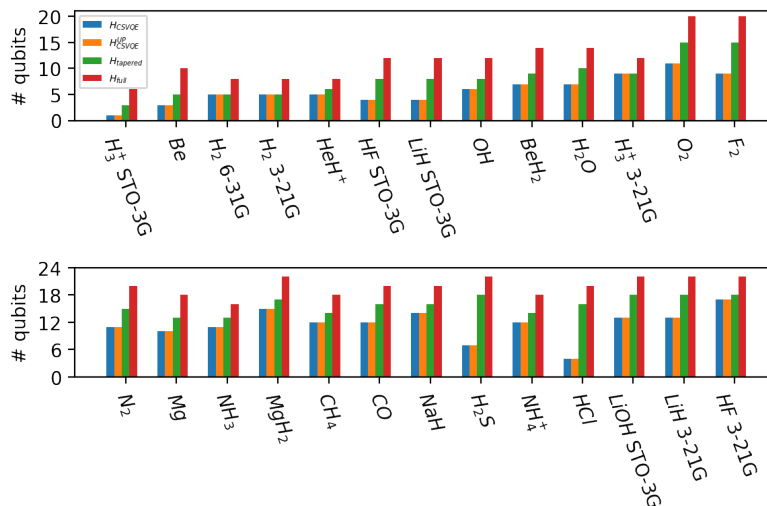


FIG. 3: Number of qubits required to simulate different electronic structure Hamiltonians in order to achieve chemical accuracy. For each molecule the full Hamiltonian, tapered Hamiltonian, CS-VQE and CS-VQE with unitary partitioning measurement reduction applied are given. Table VI in the Appendix gives numerical details of each.

Overall four Hamiltonians are generated, representing different levels of approximation, that act on 0, 1, 2 and 3 qubits respectively. The 4 qubit case represents standard VQE on the full Hamiltonian. Figure 1 summarises the error  $\Delta E$  of each of these compared to the true ground state energy (scatter plot). The number of terms in each Hamiltonian is given by the bar chart. The green and orange results have  $\mathcal{W} \equiv \mathcal{W}_{all}$  for all cases and represent the old CS-VQE implementation. For these results, in the 3 and 4 qubit Hamiltonians have an increased number of terms due to  $R_{S/LCU}$  being implemented, even though the eigenvalue of  $\mathcal{A}(\vec{r}_0)$  is not being fixed to +1. On the other hand, the grey and blue results in Figure 1 build  $U_{\mathcal{W}}$  according to Equation 11, where  $\mathcal{W} \subseteq \mathcal{W}_{all}$ . This approach ensures that  $R_{S/LCU}$  is only applied when necessary.

### C. Measurement Reduction

Figures 2 and 3 summarise the results of applying the unitary partitioning measurement reduction strategy to a set of electronic structure Hamiltonians. Here we report the number of terms and number of qubits in each Hamiltonian required to achieve chemical accuracy compared to the original problem. Appendix D gives further information about each result, where the different levels of noncontextual approximation are shown. As previously discussed in [14], even though CS-VQE in general is an approximate method, chemical accuracy can still be achieved using significantly fewer qubits. Applying unitary partitioning on-top of the reduced CS-VQE Hamiltonians required to achieve chemical accuracy can further reduce the number of terms by roughly an order of mag-

nitude. Consistent with the previous results in [30].

In Table I, we report the upper bound on the gate count required to implement measurement reduction as a sequence of rotations. The LCU method would require ancilla qubits and analysis of the circuit depth is more complicated. Further analysis can be found in [30]. The extra coherent resources required to implement unitary partitioning measurement reduction is proportional to the size of each anticommuting clique a Hamiltonian is split into [15, 30]. The sequence of rotations circuit depth scales as  $\mathcal{O}(N_s(|C|-1))$  single qubit and  $\mathcal{O}(N_s(|C|-1))$  CNOT gates, where  $N_s$  is the number of system qubits and  $|C|$  is the size of the anticommuting clique being measured. Table I reports the gate count upper bound for the largest anticommuting clique of a given CS-VQE Hamiltonian. We do not consider possible circuit simplifications, such as gate cancellations. To decrease the depth of quantum circuit required for practical application, we suggest finding nonoptimal clique covers for example if anticommuting cliques are fixed to a size of 2. The resources required to perform  $R_S$  are experimentally realistic for current and near-term devices, as only  $\mathcal{O}(N_s)$  single qubit and  $\mathcal{O}(N_s)$  CNOT gates are required [30].

The heuristic used to determine the operators in  $H_{\text{noncon}}$  selected terms in the full Hamiltonian greedily by coefficient magnitude, while keeping the set noncontextual [41]. The Hamiltonians studied here had weights dominated by diagonal Pauli operators, as the Hartree-Fock approximation accounts for most of the energy. This heavily constrains the operators allowed in  $\mathcal{A}$ . For the electronic structure Hamiltonians considered in this work, we found in all cases  $|\mathcal{A}| = 2$ . In general, we do expect more commuting terms in  $H_{\text{noncon}}$  than anticommuting terms. This is because there are more possible

commuting Pauli operators defined on  $n$  qubits compared to anticommuting operators ( $2^n$  vs  $2n+1$ ).  $\mathcal{G}$  will therefore in general be the larger contributor to the superset  $\mathcal{R}$  (Equation 5).

In Figure 2, the CS-VQE bars haven't been split into two for the case when  $R$  is constructed as  $R_{LCU}$  or  $R_S$ . This is due to  $|\mathcal{A}|$  being two in all cases, which is the special case when these operators ( $R_{LCU}$  and  $R_S$ ) end up being identical. In this instance  $R$  has the form  $R = \alpha I + i\beta P$  and thus the number of terms will only increase for every term in the Hamiltonian that  $P$  anticommutes with. However, in general  $|\mathcal{A}|$  will be greater than two and the effect of  $R$  can dramatically affect the number of terms in the resultant rotated Hamiltonian. We observe this in Fig. 1 of the Toy example, where the 2 and 3 qubit CS-VQE Hamiltonians have had  $U_{\mathcal{W}_{all}}$  applied to them even though the eigenvalue of  $A(\vec{r})$  is not fixed.

Finally, it is important to acknowledge that we only implemented the unitary partitioning measurement reduction strategy in this work. Many alternate methods have been proposed [15–28] and their effect on the number of measurements would be interesting to investigate.

#### IV. CONCLUSION

The work presented here shows that combining the unitary partitioning measurement reduction strategy with the CS-VQE algorithm can further reduce the number of terms in the projected Hamiltonian requiring separate measurement by roughly an order of magnitude for a given molecular Hamiltonian. The number of qubits needed to achieve chemical accuracy in most cases was also dramatically decreased, for example the  $\text{H}_2\text{S}$  (STO-3G singlet) problem was reduced to 7 qubits from 22.

We also improve two parts of the CS-VQE algorithm. First, we first avoid having to apply the unitary partitioning operator  $R$  after the ansatz that would avert the potential exponential increase in number of Pauli operators of the CS-VQE Hamiltonian caused by classically computing the non-Clifford rotation of the full Hamiltonian when  $R$  defined as a sequence of rotations [14, 15]. We show that applying this operation as a linear combination of unitaries [15]:  $H_{\text{full}} \mapsto H_{\text{full}}^{LCU'} = R_{LCU}^\dagger H_{\text{full}} R_{LCU}$ , results in the number terms at worst increasing quadratically with the number of qubits. This result makes classically precomputing this transformation tractable and  $R$  no longer needs to be performed coherently after the

ansatz. Secondly, we define the unitary  $U_{\mathcal{W}}$ , that maps each stabilizer in  $\mathcal{W}_{all}$  (equation 10) to a distinct single-qubit Pauli matrix, according to which stabilizer eigenvalues are fixed by the noncontextual state. This ensures the non-Clifford rotation required by CS-VQE is only applied when necessary and also reduces the number of redundant Clifford operations that are classically performed.

There are still several open questions for the CS-VQE algorithm. We summarise a few here. (1) What is the best optimization strategy to use when minimising the energy over  $(\vec{q}, \vec{r})$  in the classical noncontextual problem? (2) What heuristic is best to construct the largest  $|H_{\text{noncon}}|$ ? (3) How to efficiently determine which non-contextual stabilizers to fix while maintaining low errors? For this work, the size of each electronic structure problem allowed us to classically compute the ground state energies at each step, but if this is not possible then VQE calculations would be required. However, as each run requires fewer qubits and decreases the number of terms requiring separate measurement this approach may overall still be less costly than performing VQE over the whole problem, especially when combined with further measurement reduction strategies. (4) What are the most important terms to include in  $H_{\text{con}}$  or equivalently in  $H_{\text{noncon}}$ ? Currently, it isn't known whether  $|H_{\text{noncon}}|$  should be maximised or if selecting high priority terms [47] from the whole Hamiltonian results in a better approximation for a given problem. We leave these questions to future work.

Finally, we have written an open-source CS-VQE code that includes all the updated methodology discussed in this paper. We welcome readers to make use of this, which is freely available on GitHub at [59].

#### ACKNOWLEDGMENTS

A. R. and T.W acknowledge support from the Engineering and Physical Sciences Research Council (EP/L015242/1 and EP/S021582/1 respectively). T.W. also acknowledges support from CBKSciCon Ltd., Atos, Intel and Zapata. W.K. and P.J.L. acknowledge support by the NSF STAQ project (PHY-1818914). W. K. acknowledges support from the National Science Foundation, Grant No. DGE-1842474. P.V.C. is grateful for funding from the European Commission for VECMA (800925) and EPSRC for SEAVEA (EP/W007711/1).

- 
- [1] A. Szabo and N. S. Ostlund, *Modern quantum chemistry: introduction to advanced electronic structure theory* (Macmillan Publishing Company, New York, 2012).
- [2] A. Aspuru-Guzik, A. D. Dutoi, P. J. Love, and M. Head-Gordon, Simulated quantum computation of molecular energies, *Science* **309**, 1704 (2005).
- [3] R. Babbush, C. Gidney, D. W. Berry, N. Wiebe, J. Mc-

- Clean, A. Paler, A. Fowler, and H. Neven, Encoding electronic spectra in quantum circuits with linear t complexity, *Physical Review X* **8**, 041015 (2018).
- [4] V. E. Elfving, B. W. Broer, M. Webber, J. Gavartin, M. D. Halls, K. P. Lorton, and A. Bochevarov, How will quantum computers provide an industrially relevant computational advantage in quantum chemistry?, arXiv

- preprint arXiv:2009.12472 (2020).
- [5] A. J. McCaskey, Z. P. Parks, J. Jakowski, S. V. Moore, T. D. Morris, T. S. Humble, and R. C. Pooser, Quantum chemistry as a benchmark for near-term quantum computers, *npj Quantum Information* **5**, 1 (2019).
  - [6] A. Y. Kitaev, Quantum measurements and the abelian stabilizer problem, arXiv preprint quant-ph/9511026 (1995).
  - [7] P. J. O’Malley, R. Babbush, I. D. Kivlichan, J. Romero, J. R. McClean, R. Barends, J. Kelly, P. Roushan, A. Tranter, N. Ding, *et al.*, Scalable quantum simulation of molecular energies, *Physical Review X* **6**, 031007 (2016).
  - [8] H. Mohammadbagherpoor, Y.-H. Oh, A. Singh, X. Yu, and A. J. Rindos, Experimental challenges of implementing quantum phase estimation algorithms on ibm quantum computer, arXiv preprint arXiv:1903.07605 (2019).
  - [9] A. Peruzzo, J. McClean, P. Shadbolt, M.-H. Yung, X.-Q. Zhou, P. J. Love, A. Aspuru-Guzik, and J. L. O’Brien, A variational eigenvalue solver on a photonic quantum processor, *Nature communications* **5**, 1 (2014).
  - [10] E. Farhi, J. Goldstone, and S. Gutmann, A quantum approximate optimization algorithm, arXiv preprint arXiv:1411.4028 (2014).
  - [11] C. Bravo-Prieto, R. LaRose, M. Cerezo, Y. Subasi, L. Cincio, and P. J. Coles, Variational quantum linear solver, arXiv preprint arXiv:1909.05820 (2019).
  - [12] A. Eddins, M. Motta, T. P. Gujarati, S. Bravyi, A. Mezzacapo, C. Hadfield, and S. Sheldon, Doubling the size of quantum simulators by entanglement forging, *PRX Quantum* **3**, 010309 (2022).
  - [13] W. J. Huggins, B. A. O’Gorman, N. C. Rubin, D. R. Reichman, R. Babbush, and J. Lee, Unbiasing fermionic quantum monte carlo with a quantum computer, *Nature* **603**, 416 (2022).
  - [14] W. M. Kirby, A. Tranter, and P. J. Love, Contextual subspace variational quantum eigensolver, *Quantum* **5**, 456 (2021).
  - [15] A. Zhao, A. Tranter, W. M. Kirby, S. F. Ung, A. Miyake, and P. J. Love, Measurement reduction in variational quantum algorithms, *Physical Review A* **101**, 062322 (2020).
  - [16] A. Kandala, A. Mezzacapo, K. Temme, M. Takita, M. Brink, J. M. Chow, and J. M. Gambetta, Hardware-efficient variational quantum eigensolver for small molecules and quantum magnets, *Nature* **549**, 242 (2017).
  - [17] V. Verteletskyi, T.-C. Yen, and A. F. Izmaylov, Measurement optimization in the variational quantum eigensolver using a minimum clique cover, *The Journal of Chemical Physics* **152**, 124114 (2020).
  - [18] A. F. Izmaylov, T.-C. Yen, and I. G. Ryabinkin, Revising the measurement process in the variational quantum eigensolver: is it possible to reduce the number of separately measured operators?, *Chemical Science* **10**, 3746 (2019).
  - [19] J. Cotler and F. Wilczek, Quantum overlapping tomography, *Physical Review Letters* **124**, 100401 (2020).
  - [20] X. Bonet-Monroig, R. Babbush, and T. E. O’Brien, Nearly optimal measurement scheduling for partial tomography of quantum states, arXiv preprint arXiv:1908.05628 (2019).
  - [21] P. Gokhale and F. T. Chong,  $o(n^3)$  measurement cost for variational quantum eigensolver on molecular hamiltonians, arXiv preprint arXiv:1908.11857 (2019).
  - [22] A. Jena, S. Genin, and M. Mosca, Pauli partitioning with respect to gate sets, arXiv preprint arXiv:1907.07859 (2019).
  - [23] W. J. Huggins, J. McClean, N. Rubin, Z. Jiang, N. Wiebe, K. B. Whaley, and R. Babbush, Efficient and noise resilient measurements for quantum chemistry on near-term quantum computers, arXiv preprint arXiv:1907.13117 (2019).
  - [24] P. Gokhale, O. Angiuli, Y. Ding, K. Gui, T. Tomesh, M. Suchara, M. Martonosi, and F. T. Chong, Minimizing state preparations in variational quantum eigensolver by partitioning into commuting families, arXiv preprint arXiv:1907.13623 (2019).
  - [25] O. Crawford, B. van Straaten, D. Wang, T. Parks, E. Campbell, and S. Brierley, Efficient quantum measurement of pauli operators in the presence of finite sampling error, *Quantum* **5**, 385 (2021).
  - [26] H.-Y. Huang, R. Kueng, and J. Preskill, Predicting many properties of a quantum system from very few measurements, *Nature Physics* **16**, 1050 (2020).
  - [27] C. Hadfield, S. Bravyi, R. Raymond, and A. Mezzacapo, Measurements of quantum hamiltonians with locally-biased classical shadows, arXiv preprint arXiv:2006.15788 (2020).
  - [28] H.-Y. Huang, R. Kueng, and J. Preskill, Efficient estimation of pauli observables by derandomization, *Physical Review Letters* **127**, 030503 (2021).
  - [29] A. F. Izmaylov, T.-C. Yen, R. A. Lang, and V. Verteletskyi, Unitary partitioning approach to the measurement problem in the variational quantum eigensolver method, *Journal of Chemical Theory and Computation* **16**, 190 (2020).
  - [30] A. Ralli, P. J. Love, A. Tranter, and P. V. Coveney, Implementation of measurement reduction for the variational quantum eigensolver, *Physical Review Research* **3**, 033195 (2021).
  - [31] S. Kochen and E. P. Specker, The problem of hidden variables in quantum mechanics, in *The logico-algebraic approach to quantum mechanics* (Springer, 1975) pp. 293–328.
  - [32] C. Budroni, Contextuality, memory cost and non-classicality for sequential measurements, *Philosophical Transactions of the Royal Society A* **377**, 20190141 (2019).
  - [33] C. Budroni, A. Cabello, O. Gühne, M. Kleinmann, and J.-Å. Larsson, Quantum contextuality, arXiv preprint arXiv:2102.13036 (2021).
  - [34] N. de Silva, Graph-theoretic strengths of contextuality, *Physical Review A* **95**, 032108 (2017).
  - [35] A. Cabello, Converting contextuality into nonlocality, *Physical Review Letters* **127**, 070401 (2021).
  - [36] M. Howard, J. Wallman, V. Veitch, and J. Emerson, Contextuality supplies the ‘magic’ for quantum computation, *Nature* **510**, 351 (2014).
  - [37] N. D. Mermin, Simple unified form for the major non-hidden-variables theorems, *Physical review letters* **65**, 3373 (1990).
  - [38] J. S. Bell, On the einstein podolsky rosen paradox, *Physics Physique Fizika* **1**, 195 (1964).
  - [39] A. Peres, Incompatible results of quantum measurements, *Physics Letters A* **151**, 107 (1990).
  - [40] R. W. Spekkens, Quasi-quantization: Classical statistical theories with an epistemic restriction, in *Quantum*

- Theory: Informational Foundations and Foils*, edited by G. Chiribella and R. W. Spekkens (Springer Netherlands, Dordrecht, 2016) pp. 83–135.
- [41] W. M. Kirby and P. J. Love, Classical simulation of non-contextual pauli hamiltonians, *Physical Review A* **102**, 032418 (2020).
- [42] R. W. Spekkens, Evidence for the epistemic view of quantum states: A toy theory, *Physical Review A* **75**, 032110 (2007).
- [43] R. W. Spekkens, Quasi-quantization: classical statistical theories with an epistemic restriction, in *Quantum Theory: Informational Foundations and Foils* (Springer, 2016) pp. 83–135.
- [44] T. J. Weaving, A. Ralli, W. M. Kirby, A. Tranter, P. J. Love, and P. V. Coveney, A stabilizer framework for contextual subspace vqe and the noncontextual projection ansatz, arXiv preprint arXiv:2204.02150 (2022).
- [45] R. Raussendorf, J. Bermejo-Vega, E. Tyhurst, C. Okay, and M. Zurel, Phase-space-simulation method for quantum computation with magic states on qubits, *Physical Review A* **101**, 012350 (2020).
- [46] M. A. Nielsen and I. L. Chuang, *Quantum computation and quantum information: 10th anniversary edition* (Cambridge University Press, 2011) pp. 454–459.
- [47] D. Poulin, M. B. Hastings, D. Wecker, N. Wiebe, A. C. Doherty, and M. Troyer, The trotter step size required for accurate quantum simulation of quantum chemistry, arXiv preprint arXiv:1406.4920 (2014).
- [48] J. Dehaene and B. De Moor, Clifford group, stabilizer states, and linear and quadratic operations over  $GF(2)$ , *Physical Review A* **68**, 042318 (2003).
- [49] A. M. Childs and N. Wiebe, Hamiltonian simulation using linear combinations of unitary operations, *Quantum Info. Comput.* **12**, 901 (2012).
- [50] G. H. Low and I. L. Chuang, Hamiltonian Simulation by Qubitization, *Quantum* **3**, 163 (2019).
- [51] D. W. Berry, A. M. Childs, R. Cleve, R. Kothari, and R. D. Somma, Exponential improvement in precision for simulating sparse hamiltonians, in *Proceedings of the 46th Annual ACM Symposium on Theory of Computing* (Association for Computing Machinery, 2014) pp. 283–292.
- [52] L. K. Grover, Quantum mechanics helps in searching for a needle in a haystack, *Physical Review Letters* **79**, 325 (1997).
- [53] G. G. Guerreschi, Repeat-until-success circuits with fixed-point oblivious amplitude amplification, *Physical Review A* **99**, 022306 (2019).
- [54] M. Boyer, G. Brassard, P. Hoyer, and A. Tapp, Tight bounds on quantum searching, *Fortschritte der Physik: Progress of Physics* **46**, 493 (1998).
- [55] S. Bravyi, J. M. Gambetta, A. Mezzacapo, and K. Temme, Tapering off qubits to simulate fermionic hamiltonians, arXiv preprint arXiv:1701.08213 (2017).
- [56] W. M. Kirby, ContextualSubspaceVQE, <https://github.com/wmkirby1/ContextualSubspaceVQE> (2021).
- [57] A. A. Hagberg, D. A. Schult, and P. J. Swart, Exploring network structure, dynamics, and function using networkx, in *Proceedings of the 7th Python in Science Conference*, edited by G. Varoquaux, T. Vaught, and J. Millman (Pasadena, CA USA, 2008) pp. 11 – 15.
- [58] D. J. Welsh and M. B. Powell, An upper bound for the chromatic number of a graph and its application to timetabling problems, *The Computer Journal* **10**, 85 (1967).
- [59] A. Ralli and T. J. Weaving, symmer, <https://github.com/UCL-CCS/symmer> (2022).
- [60] W. M. Kirby and P. J. Love, Contextuality test of the nonclassicality of variational quantum eigensolvers, *Physical review letters* **123**, 200501 (2019).
- [61] J. R. McClean, N. C. Rubin, K. J. Sung, I. D. Kivlichan, X. Bonet-Monroig, Y. Cao, C. Dai, E. S. Fried, C. Gidney, B. Gimby, *et al.*, Openfermion: the electronic structure package for quantum computers, *Quantum Science and Technology* **5**, 034014 (2020).
- [62] D. Wagner, K. Weihe, E. Ihler, D. Wagner, F. Wagner, J. Gustedt, and M. Morvan, A linear time algorithm for edge-disjoint paths in, in *Proc. of the First Annual European Symposium on Algorithms*, Vol. 8 (Springer) pp. 625–712.

### Appendix A: “Peres-Mermin Square”

The “Peres-Mermin square” [37, 39] involves the construction of nine measurements arranged in a square. In this section we follow the construction given in [33]. Each measurement has only two possible outcomes (dichotomic) +1 and -1. In a realistic interpretation, performing each measurement on an object reveals whether the property is present (+1) or absent (-1), yielding nine properties.

We take three measurements along a column or row to form a “context” - a set of measurements whose values can be jointly measured i.e. the observables commute and thus share a common eigenbasis. Table II gives an example.

IZ	ZI	ZZ	$r_0$
XI	IX	XX	$r_1$
XZ	ZX	YY	$r_2$
$c_0$	$c_1$	$c_2$	

TABLE II: Example Peres-Mermin square of nine possible observables for a physical system, where each measurement can be assigned a  $\pm 1$  value.

In a classical (noncontextual) model for this system, the nine measurements  $\{IZ, ZI, ZZ, XI, IX, XX, XZ, ZX, YY\}$  can be assigned a definite value independent of the context the measurement is obtained in. For example if all measurements are assigned +1 in Table II, then  $c_0 = c_1 = c_2 = r_0 = r_1 = r_2 = +1$  and six positive products are obtained. If a single entry in Table II is changed it will affect two products (a row and column product). We consider the following Equation in this setting:

$$\begin{aligned}
 \langle PM \rangle &\equiv \langle IZ \cdot ZI \cdot ZZ \rangle + \langle XI \cdot IX \cdot XX \rangle + \langle XZ \cdot ZX \cdot YY \rangle + \langle IZ \cdot XI \cdot XZ \rangle + \langle ZI \cdot IX \cdot ZX \rangle - \langle ZZ \cdot XX \cdot YY \rangle \\
 &= r_0 + r_1 + r_2 + c_0 + c_1 - c_2
 \end{aligned}
 \tag{A1}$$

and find that classically we get an inequality  $\langle PM \rangle \leq 4$ . We reiterate that this is the setting of eight +1 assignments and a single -1 assignment. This inequality is saturated when the -1 value is assigned to one of the observables in the last column of Table II.

The significance of this inequality is that it can be violated by quantum systems. Thinking of this in a quantum setting, the operators in rows and columns of Table II commute. If we multiply along the rows and columns we get  $+II$  apart from the last column where  $c_2 = -II$  (see Table III). This is the case regardless of what quantum state is considered. Using the expectation values of the product of these operators in Equation A1, we find  $\langle PM \rangle = 6$ , violating the classical bound.

IZ	ZI	ZZ	$\langle +II \rangle = +1$
XI	IX	XX	$\langle +II \rangle = +1$
XZ	ZX	YY	$\langle +II \rangle = +1$
$\langle +II \rangle = +1$	$\langle +II \rangle = +1$	$\langle -II \rangle = -1$	

TABLE III: Example Peres-Mermin square of nine Hermitian operators, all with  $\pm 1$  eigenvalues - representing observables.

Classically Equation A1 is bounded as  $\langle PM \rangle \leq 4$  due to the assumption that the nine observables of the object can be assigned a value consistently. Violation of this bound implies that either the value assignment must depend on which context (row or column) the observable appears in or there is no value assignment. This phenomenon is known as quantum contextuality [33].

In VQE, a Hamiltonian is defined by a linear combination of Pauli operators. The expectation value is obtained by measuring each Pauli operator in a separate experiment and combining the results. Different groups of commuting operators form contexts. In general there will be incompatible contexts where it is impossible to consistently assign joint outcomes. In other words, different inference relations will lead to contradictions. Outcomes assigned to individual measurements are therefore context-dependent and the problem is contextual. If not, then the problem is noncontextual and a noncontextual hidden variable model can be used to solve such systems.

---

**Algorithm 1** Test for strong contextuality in a given set of Pauli operators [60]

---

**Input:**  $\mathcal{P} = \{P_0, P_1, P_2, \dots\}$  ▷ Input  $\mathcal{P}$  is a set of Pauli operators.  
**Output:** *contextual* (*True/False*) ▷ Whether the set  $\mathcal{P}$  is strongly contextual.

$\mathcal{Z} \leftarrow \{\}$   
 $\mathcal{T} \leftarrow \{\}$   
*contextual*  $\leftarrow$  *False*

**for**  $i = 0$  to  $|\mathcal{P}| - 1$  **do**  
  **if**  $[P_i, P_j] = 0 \forall j \neq i$  where  $j = 0$  to  $|\mathcal{P}| - 1$  **then**  
     $\mathcal{Z} \leftarrow \mathcal{Z} \cup \{P_i\}$   
  **else**  
     $\mathcal{T} \leftarrow \mathcal{T} \cup \{P_i\}$   
  **end if**  
**end for**

**for**  $i = 0$  to  $|\mathcal{T}| - 3$  **do**  
  **for**  $j = i + 1$  to  $|\mathcal{T}| - 2$  **do**  
    **for**  $k = j + 1$  to  $|\mathcal{T}| - 1$  **do**  
      **if**  $[P_i, P_j] = 0, [P_i, P_k] = 0$  and  $\{P_j, P_k\} = 0$  **then**  
        *contextual*  $\leftarrow$  *True*  
        **return** *contextual*  
      **else**  
        **continue**  
      **end if**  
    **end for**  
  **end for**  
**end for**  
**return** *contextual*

---

## Appendix B: Contextual-Subspace VQE overview

In the following subsections we summarise all the details required to implement the CS-VQE algorithm, where a problem Hamiltonian is split into a contextual and noncontextual part [14]:

$$H_{\text{full}} = H_{\text{con}} + H_{\text{noncon}}. \tag{B1}$$

### 1. Noncontextual Part

#### a. Testing for contextuality

Let  $\mathcal{S}^{H_{\text{full}}}$  be the set of Pauli operators, in the full system Hamiltonian, requiring measurement in a VQE experiment. It was shown in [45, 60], that a set of four Pauli operators  $\{A, B, C, D\}$  is strongly contextual if  $A$  commutes with both  $B$  and  $C$ , but  $B$  anticommutes with  $C$ . If this condition is not present, then the set is noncontextual.

Given an arbitrary set of Pauli operators  $\mathcal{P}$ , this gives an algorithm to check for contextuality [60]. A pseudo algorithm is given in algorithm 1. First an  $\mathcal{O}(|\mathcal{P}|^2)$  routine is used to remove completely commuting operators  $\mathcal{Z}$ , leaving the remaining set  $\mathcal{T}$ . Then a procedure taking  $\mathcal{O}(|\mathcal{T}|^3)$  steps is used to determine whether  $\mathcal{P}$  is contextual. This check for contextuality is implemented in OpenFermion [61].

b. *Obtaining Noncontextual Hamiltonian*

To begin CS-VQE, we first need to define the contextual and noncontextual parts. The task of finding the largest noncontextual subset of Pauli operators in  $\mathcal{S}^{H_{\text{full}}}$  is a generalization of the disjoint cliques problem [41, 62], which is NP-complete. However, different heuristics can be used to approximately solve this problem.

To date, VQE experiments have mainly focused on chemistry Hamiltonians, where Hartree-Fock accounts for most of the energy. Such Hamiltonians contain Pauli operators that  $l_1$  norms are dominated by diagonal terms - Pauli operators made up of tensor products of single qubit  $I$  and Pauli  $Z$  matrices. To find a noncontextual set in such a scenario, a greedy heuristic selecting high weight terms from the full Hamiltonian first can be used, while checking the set remains noncontextual using algorithm 1. This gives a noncontextual set containing mainly diagonal terms, with some additional operators [41]. Alternative procedures to find the largest noncontextual subsets remain an open question for the CS-VQE algorithm.

c. *Noncontextual hidden variable model*

Once the noncontextual Hamiltonian  $H_{\text{noncon}}$  is determined, we can define the set  $\mathcal{S}^{H_{\text{noncon}}}$  to be the Pauli operators in  $H_{\text{noncon}}$ . We split  $\mathcal{S}^{H_{\text{noncon}}}$  into two subsets  $\mathcal{Z}$  and  $\mathcal{T}$  - representing the set of universally commuting Pauli operators  $\mathcal{Z}$  and their complement respectively [14, 41]:

$$\mathcal{S}^{H_{\text{noncon}}} = \mathcal{Z} \cup \mathcal{T} = \left\{ \bigcup_{\substack{i=0 \\ \forall P_i \in \mathcal{Z}}}^{|\mathcal{Z}|-1} P_i \right\} \cup \left\{ \bigcup_{\substack{i=0 \\ \forall P_i \in \mathcal{T}}}^{|\mathcal{T}|-1} P_i \right\}. \quad (\text{B2})$$

Slight modifications to Algorithm 1 achieve this - where  $\mathcal{P}$  would be set to be  $\mathcal{S}^{H_{\text{noncon}}}$  and both  $\mathcal{Z}, \mathcal{T}$  should be returned.

The operators in  $\mathcal{Z}$  are noncontextual, as by definition they are universally commuting and represent symmetries of  $H_{\text{noncon}}$ . For the overall super-set  $\mathcal{S}^{H_{\text{noncon}}}$  to be noncontextual, the remaining operators in  $\mathcal{T}$  must be made up of  $N$  disjoint cliques  $C_j$  [41], where operators within a clique must all commute with each other and operators between cliques pairwise anticommute. This is because commutation forms an equivalence relation on  $\mathcal{T}$  if and only if  $\mathcal{S}^{H_{\text{noncon}}}$  is noncontextual [14, 41, 45]. We can write  $\mathcal{T}$  as:

$$\mathcal{T} = \bigcup_{\substack{i=0 \\ \forall P_i \in \mathcal{T}}}^{|\mathcal{T}|-1} P_i = \bigcup_{j=0}^{N-1} C_j = \bigcup_{j=0}^{N-1} \left( \bigcup_{\substack{k=0 \\ \text{where} \\ [P_k, P_i]=0 \\ \forall P_k, P_i \in C_j}}^{|C_j|-1} P_k^{(j)} \right). \quad (\text{B3})$$

We re-define each clique  $C_j$  using the identity operation defined by the first operator of the  $j$ th clique,  $P_0^{(j)} P_0^{(j)} = \mathcal{I}$ , which represents of the first operator in each of the  $N$  cliques. We write the  $j$ th clique as [41]:

$$C_j = \bigcup_{\forall P_k \in C_j} P_k^{(j)} = \bigcup_{\forall P_k \in C_j} P_k^{(j)} P_0^{(j)} P_0^{(j)} = \bigcup_{\forall P_k \in C_j} \left( P_k^{(j)} P_0^{(j)} \right) P_0^{(j)} = \bigcup_{k=0}^{|C_j|-1} A_k^{(j)} P_0^{(j)} \quad (\text{B4})$$

The new operators  $A_k^{(j)} = P_k^{(j)} P_0^{(j)}$  are just Pauli operators up to a complex phase. The new operators  $A_k^{(j)}$  must still commute with the universally commuting operators in  $\mathcal{Z}$ , but now must also commute with all the other terms in the  $N - 1$  cliques  $C_j$  [41]. Using this, the noncontextual set (Equation B2) can be rewritten as:

$$\mathcal{S}^{H_{\text{noncon}}} = \left\{ \bigcup_{\substack{i=0 \\ \forall P_i \in \mathcal{Z}}}^{|\mathcal{Z}|-1} P_i \right\} \cup \left\{ \bigcup_{j=0}^{N-1} C_j \right\} \quad (\text{B5a})$$

$$= \underbrace{\left\{ \bigcup_{\substack{i=0 \\ \forall P_i \in \mathcal{Z}}}^{|\mathcal{Z}|-1} P_i \right\}}_{\mathcal{Z}} \cup \underbrace{\left\{ \bigcup_{j=0}^{N-1} \left( \bigcup_{\substack{k=0 \\ \text{where} \\ [P_k, P_l]=0 \\ \forall P_k, P_l \in C_j}}^{|C_j|-1} A_k^{(j)} P_0^{(j)} \right) \right\}}_{\mathcal{T}}. \quad (\text{B5b})$$

So far we have considered the noncontextual set of Pauli operators  $\mathcal{S}^{H_{\text{noncon}}}$ , which in general will be a dependent set. By this we mean that some operators in the set can be written as a product of other commuting operators in the set. We need to reduce this set  $\mathcal{S}^{H_{\text{noncon}}}$  to an independent set of Pauli operators, where all operators in the noncontextual Hamiltonian can be inferred from the values of other operators in the set under the Jordan product.

To obtain an independent set from  $\mathcal{S}^{H_{\text{noncon}}}$ , we first take the completely commuting Pauli operators:

$$\begin{aligned} \mathcal{G}' &\equiv \mathcal{Z} \cup \left\{ \bigcup_{j=0}^{N-1} \{A_k^{(j)} | k = 1, 2, \dots, |C_j| - 1\} \right\} \\ &\equiv \left\{ \bigcup_{\substack{i=0 \\ \forall P_i \in \mathcal{Z}}}^{|\mathcal{Z}|-1} P_i \right\} \cup \left\{ \bigcup_{j=0}^{N-1} \{A_k^{(j)} | k = 1, 2, \dots, |C_j| - 1\} \right\}, \end{aligned} \quad (\text{B6})$$

and using the procedure in [46] find an independent subset  $\mathcal{G}$ :

$$\mathcal{G} \equiv \{P_i | i = 0, 1, \dots, |\mathcal{G}| - 1\}. \quad (\text{B7})$$

Appendix C in [41] gives all steps required.

Finally, we need to consider the  $N$  pairwise anticommuting  $P_0^{(j)}$  operators defined by the  $N$  anticommuting cliques. As the operators in  $\mathcal{G}$  universally commute with all operators in the noncontextual Hamiltonian, each operator in the set  $\{P_0^{(j)} | j = 0, 1, \dots, (N-1)\}$  must be independent of  $\mathcal{G}$  under the Jordan product [41]. Combining these results, we get the set  $\mathcal{R}$ :

$$\mathcal{R} \equiv \{P_0^{(j)} | j = 0, 1, \dots, N-1\} \cup \mathcal{G} \quad (\text{B8})$$

Inspecting the properties of  $\mathcal{R}$ , one can bound its size. The set  $\mathcal{G}$  has size at most  $n-1$ , as  $n$  independent commuting Pauli operators form a complete commuting set of observables for  $n$  qubits. In other words, as  $\mathcal{G}$  is a universally commuting set, if its size was  $n$  (or more) then taking  $\mathcal{G}$  and one operator  $P_0^{(j)}$  (the set  $\mathcal{G} \cup \{P_0^{(j)}\}$ ) is also a fully commuting set - and would be a commuting set of size  $n+1$  (or more) [41]. The maximum number of independent anticommuting operators on  $n$  qubits was shown in [45] to be  $2n+1$ . This actually bounds the size of  $\mathcal{R}$ , which occurs when the set  $\mathcal{G}$  (and thus  $\mathcal{Z}$ ) is empty [41].

Looking at the noncontextual set of Pauli operators Equation B5, making up the  $H_{\text{noncon}}$ , we see that the subset  $\mathcal{G}$  in  $\mathcal{R}$  (Equation B8) includes all the generators for the terms in  $\mathcal{Z}$  and each Pauli  $A_k^{(j)}$  operator. Any operator in  $\mathcal{Z}$  and each Pauli  $A_k^{(j)}$  operator can therefore be found by a finite combination of operators in  $\mathcal{G}$ . Each operator in  $\mathcal{T}$  can also be generated by a combination of one  $P_0^{(j)}$  operator and some combination of operators in  $\mathcal{G}$ . Again  $\mathcal{R}$  (Equation B8) contains all the operators required. To summarise, the set  $\mathcal{R}$  contains all the required terms to reproduce the expectation value of any operator in  $\mathcal{S}^{H_{\text{noncon}}}$  under the Jordan product.

We have shown how the Pauli operators making  $H_{\text{noncon}}$  can be simultaneously assigned definite values without contradiction. This allows the introduction of a phase-space description of the eigenspace of  $H_{\text{noncon}}$  [41]. Next we will introduce what this phase-space model is in the context of this work.

A joint value assignment of  $\pm 1$  to each operator in  $\mathcal{R}$  represents the ontic state of the physical system. Probability distributions corresponding to valid quantum states must obey an uncertainty relation [41, 43]. To enforce these two conditions are sufficient. (1) The commuting generators  $\mathcal{G}$  have definite values and (2) the expectation values for the  $P_0^{(j)}$  terms form a unit vector [41]. In this frame, our noncontextual state is defined as [41]:

$$(\vec{q}, \vec{r}) = (q_0, q_1, \dots, q_{|\mathcal{G}|-1}, r_0, r_1, \dots, r_{N-1}). \quad (\text{B9})$$

With respect to the phase-space model [41], a valid noncontextual state  $(\vec{q}, \vec{r})$  sets the expectation value of the operators in  $\mathcal{R}$ , where  $\langle G_i \rangle = q_i = \pm 1$  and  $\langle P_0^{(j)} \rangle = r_j$  such that  $(\sum_{j=0}^{N-1} |r_j|^2)^{1/2} = 1$ .

It was shown in [41] that probabilities for outcomes  $G_i$  and  $P_0^{(j)}$  should be obtained as the marginals of:

$$P(p_{j=0}, p_{j=1}, \dots, p_{j=(N-1)}, g_0, g_1, \dots, g_{|\mathcal{G}|-1}) = \left( \prod_{i=0}^{|\mathcal{G}|-1} \delta_{g_i, q_i} \right) \left( \prod_{j=0}^{N-1} \frac{1}{2} |p_j + r_j| \right). \quad (\text{B10})$$

Further analysis is given in [41].

In summary, a noncontextual state is fully defined by  $(\vec{q}, \vec{r})$  which determines all the expectation values of the operators in  $\mathcal{R}$  (Equation B8), where  $\langle G_i \rangle = q_i \in \{-1, +1\}$  and  $\langle P_0^{(j)} \rangle = r_j$ . We summarise this as:

$$\underbrace{\{ \underbrace{\langle P_0^{(0)} \rangle}_{r_0}, \underbrace{\langle P_0^{(1)} \rangle}_{r_1}, \dots, \underbrace{\langle P_0^{(N-1)} \rangle}_{r_{N-1}} \}}_{\vec{r}} \text{ and } \underbrace{\{ \underbrace{\langle G_0 \rangle}_{q_0}, \underbrace{\langle G_1 \rangle}_{q_1}, \dots, \underbrace{\langle G_{|\mathcal{G}|-1} \rangle}_{q_{|\mathcal{G}|-1}} \}}_{\vec{q}}. \quad (\text{B11})$$

The expectation value of all the operators in  $\mathcal{S}^{H_{\text{noncon}}}$  are generated from some finite combination of terms in  $\mathcal{R}$  under the Jordan product. This by extension will induce the expectation value for  $H_{\text{noncon}}$ . Explicitly, let  $P_i^{\mathcal{Z}} \in \mathcal{Z} \subseteq \mathcal{S}^{H_{\text{noncon}}}$  then if we let  $\mathcal{J}_{P_i^{\mathcal{Z}}}^{\mathcal{G}}$  be the set of indices such that  $P_i^{\mathcal{Z}} = \prod_{i \in \mathcal{J}_{P_i^{\mathcal{Z}}}^{\mathcal{G}}} G_i$ ; then [41]:

$$\langle P_i^{\mathcal{Z}} \rangle = \prod_{i \in \mathcal{J}_{P_i^{\mathcal{Z}}}^{\mathcal{G}}} \langle G_i \rangle = \prod_{i \in \mathcal{J}_{P_i^{\mathcal{Z}}}^{\mathcal{G}}} q_i. \quad (\text{B12})$$

In words, we combine the expectation value of some finite set of Pauli operators in the independent set  $\mathcal{G}$  - given by  $\mathcal{J}_{P_i^{\mathcal{Z}}}^{\mathcal{G}}$  - to reproduce the expectation value for  $\langle P_i^{\mathcal{Z}} \rangle$ .

Similarly, the expectation value for each  $A_k^{(j)} P_0^{(j)} \in \mathcal{T} \subseteq \mathcal{S}^{H_{\text{noncon}}}$  (Equation B5) term is given by:

$$\langle A_i^{(j), \in \mathcal{G}} P_0^{(j), \in \mathcal{T}} \rangle = \left( \prod_{i \in \mathcal{J}_{A_i^{(j)}}^{\mathcal{G}}} \langle G_i \rangle \right) r_j = \left( \prod_{i \in \mathcal{J}_{A_i^{(j)}}^{\mathcal{G}}} q_i \right) r_j, \quad (\text{B13})$$

where  $\mathcal{J}_{A_i^{(j)}}^{\mathcal{G}}$  are the set of indices such that  $\langle A_i^{(j)} \rangle = \prod_{i \in \mathcal{J}_{A_i^{(j)}}^{\mathcal{G}}} \langle G_i \rangle$  and  $\langle P_0^{(j)} \rangle = r_j$  [41].

We can write the noncontextual Hamiltonian as:

$$H_{\text{noncon}} = \left( \sum_{i=0}^{|\mathcal{Z}|-1} c_i P_i^{\mathcal{Z}} \right) + \sum_{j=0}^{N-1} \left[ \sum_{k=0}^{|\mathcal{C}_j|-1} a_k A_k^{(j)} P_0^{(j)} \right] \quad (\text{B14})$$

and find the energy by:

$$\langle H_{\text{noncon}} \rangle = E_{\text{noncon}}(\vec{q}, \vec{r}) = \left( \sum_{i=0}^{|\mathcal{Z}|-1} \beta_i \langle P_i^{\mathcal{Z}} \rangle \right) + \sum_{j=0}^{N-1} \left[ \sum_{k=0}^{|\mathcal{C}_j|-1} \beta_k \langle A_k^{(j)} P_0^{(j)} \rangle \right], \quad (\text{B15})$$

where  $\beta_i$  and  $\beta_k$  are real coefficients and each expectation value is given by Equation B12 and B13 [41].

d. Solving the Noncontextual Hamiltonian

To find the ground state of  $H_{\text{noncon}}$ , we minimize Equation B15 via a brute-force search as described in [41]. Algorithm 2 summarises the steps. This could be done in the work presented here, because  $\mathcal{R}$  was small for all molecular systems considered. First a trial  $\vec{q}$  is defined. This is a set of  $\pm 1$  expectation values for each  $G_j$ . An initial guess of the amplitudes  $r_i$  of the unit vector  $\vec{r}$  is made and the energy (Equation B15) is minimized over this continuous parameterization of  $\vec{r}$  for a fixed trial  $\vec{q}$ , until the energy converges to a minimum. These steps are repeated for all the  $2^{|\mathcal{G}|}$  assignments of  $\vec{q}$ . The  $(\vec{q}, \vec{r})$  combination that gives the lowest overall energy represents the noncontextual ground state of the physical system. In the main text we denote this parameterization as  $(\vec{q}_0, \vec{r}_0)$ . Note for a fixed  $\vec{q}$ , we optimize over  $\vec{r}$ . This can be thought of as optimizing a function defined on a hypersphere. Currently we haven't explored the properties of this function.

It remains an open question for the CS-VQE algorithm if alternate optimization strategies are possible, for example using chemical intuition during optimization. This brute force approach of searching over all  $2^{|\mathcal{G}|}$  possibilities for  $\vec{q}$  may not be necessary. In the next section, we discuss how to map the contextual problem into a subspace consistent with a defined noncontextual state  $(\vec{q}, \vec{r})$ .

---

**Algorithm 2** Brute force method to solve noncontextual problem

---

```

 $\mathcal{Q} \leftarrow \{q_0, q_1, \dots, q_{|\mathcal{G}|-1}\}^{2^{|\mathcal{G}|}}$  ▷ Set  $\mathcal{Q}$  contains all possible  $\vec{q}$  vectors, where  $q_i \in \{+1, -1\}$ .

2:  $\vec{q}_0 \leftarrow \{\}$ 
    $\vec{r}_0 \leftarrow \{\}$ 
4:  $E_{\text{noncon}}^0 \leftarrow 0$ 

   for  $\vec{q}_{\text{test}}$  in  $\mathcal{Q}$  do
6:    $\vec{r}_{\text{opt}}, E_{\text{noncon}}^{\text{opt}} \leftarrow \underset{\vec{r}}{\text{argmin}}[E_{\text{noncon}}(\vec{q}_{\text{test}}, \vec{r})]$  ▷ for a given  $\vec{q}_{\text{test}}$ , minimize the energy (Equation B15) with respect to  $\vec{r}$ .
       if  $E_{\text{noncon}}^{\text{opt}} < E_{\text{noncon}}^0$  then
8:          $\vec{q}_0 \leftarrow \vec{q}_{\text{test}}$ 
            $\vec{r}_0 \leftarrow \vec{r}_{\text{opt}}$ 
10:         $E_{\text{noncon}}^0 \leftarrow E_{\text{noncon}}^{\text{opt}}$ 
       else
12:         continue
       end if
14: end for

return  $\vec{q}_0, \vec{r}_0, E_{\text{noncon}}^0$ 

```

---

## 2. Mapping to contextual subspace

In section IIE of the main text, the full Hamiltonian is mapped contextual subspace consistent with the noncontextual ground state by implementing  $U_{\mathcal{W}}$  (Equation 11) followed by projecting the rotated Hamiltonian with  $Q_{\mathcal{W}}$ . However, the definitions for the operators making up  $U_{\mathcal{W}}$  were omitted. This subsection gives these details and is split into three parts. The first two parts consider how  $R$  is constructed. This is the problem of mapping a linear combination of pairwise anticommuting Pauli operators to a single Pauli operator and is known as unitary partitioning [15, 29]. In the context of this work, we use this to define  $R$  such that  $RA(\vec{r})R^\dagger \mapsto P_0^{(k)}$ . In the original formulation of CS-VQE only the sequence of rotations construction of  $R$  is used in the algorithm. We provide an alternative approach using the linear combination of unitaries construction proposed in [15], which results in superior scaling. We show the effect each conjugate rotation  $R$  has on the number of terms in a given qubit Hamiltonian. The last subsection gives the unitary rotations required to map a commuting set of Pauli operators to single qubit Pauli  $Z$  operators.

In each of these subsections, we use the notation that Pauli operators with multiple indices represent the multiplication of Pauli operators:  $P_a P_b P_c = P_{abc}$ . These terms will also be Pauli operators up to a complex phase.

a. Unitary partitioning via a sequence of rotations

In this subsection, we show how  $A(\vec{r}) \mapsto P_0^{(k)} = R_S A(\vec{r}) R_S^\dagger$ , where  $R_S$  is defined by a sequence of rotations [15, 30]. Given the set of anticommuting operators  $A(\vec{r})$  (Equation 6), we can define the following self-inverse operators:

$$\{\mathcal{X}_{kj} = iP_0^{(k)} P_0^{(j)} \quad \forall P_0^{(j)} \in \mathcal{A} \text{ where } j \neq k\}, \quad (\text{B16})$$

where  $P_0^{(k)} \in \mathcal{A}$ . To simplify the notation we drop the subscript 0 (denoting the first operator in a clique) and write each  $P_0^{(k)}$ ,  $P_0^{(j)}$  as  $P_k$  and  $P_j$  respectively.

The adjoint rotation generated by one of these operator  $\mathcal{X}_{kj}$  operators will be:

$$\begin{aligned} e^{-i\frac{\theta_{kj}}{2}\mathcal{X}_{kj}} A(\vec{r}) e^{+i\frac{\theta_{kj}}{2}\mathcal{X}_{kj}} &= R_{S_{kj}}(\theta_{kj}) A(\vec{r}) R_{S_{kj}}^\dagger(\theta_{kj}) \\ &= (r_j \cos \theta_{kj} - r_k \sin \theta_{kj}) P_j + (\beta_j \sin \theta_{kj} + r_k \cos \theta_{kj}) P_k + \sum_{\substack{P_l \in \mathcal{A} \\ \forall l \neq k, j}} \beta_l P_l. \end{aligned} \quad (\text{B17})$$

The coefficient of  $P_j$  can be made to go to 0, by setting  $r_j \cos \theta_{kj} = r_k \sin \theta_{kj}$ . This approach removes the term with index  $j$  and increases the coefficient of  $P_k$  from  $r_k \mapsto \sqrt{r_k^2 + r_j^2}$  [15]. This process is repeated over all indices excluding  $j = k$  until only the  $P_k$  term remains. This procedure can be concisely written using the following operator [15]:

$$R_S = \prod_{\substack{j=0 \\ \forall j \neq k}}^{|\mathcal{A}|-1} e^{-i\frac{\theta_{kj}}{2}\mathcal{X}_{kj}} = \prod_{\substack{j=0 \\ \forall j \neq k}}^{|\mathcal{A}|-1} R_{S_{kj}}(\theta_{kj}) = \prod_{\substack{j=0 \\ \forall j \neq k}}^{|\mathcal{A}|-1} \left[ \cos\left(\frac{\theta_{kj}}{2}\right) \mathcal{I} - i \sin\left(\frac{\theta_{kj}}{2}\right) \mathcal{X}_{kj} \right], \quad (\text{B18})$$

which is simply a sequence of rotations. The angle  $\theta_{kj}$  is defined recursively at each step of the removal process, as the coefficient of  $P_k$  increases at each step and thus must be taken into account. The correct solution for  $\theta_{kj}$  must be chosen given the signs of  $r_k$  and  $r_k$  [15]. The overall action of this sequence of rotations is:

$$R_S A(\vec{r}) R_S^\dagger = P_k. \quad (\text{B19})$$

Looking at Equation B18, expanding the product of rotations results in  $R_S$  containing  $\mathcal{O}(2^{|\mathcal{A}|-1})$  Pauli operators. We write this operator as:

$$R_S = \sum_b^{\mathcal{O}(2^{|\mathcal{A}|-1})} \delta_b P_b. \quad (\text{B20})$$

The adjoint rotation of  $R_S$  on a general Hamiltonian  $H_q = \sum_a^{|H_q|} c_a P_a$  is:

$$\begin{aligned} R_S H_q R_S^\dagger &= \left( \sum_b^{\mathcal{O}(2^{|\mathcal{A}|-1})} \delta_b P_b \right) \sum_a^{|H_q|} c_a P_a \left( \sum_c^{\mathcal{O}(2^{|\mathcal{A}|-1})} \delta_c^* P_c \right) \\ &= \sum_b^{\mathcal{O}(2^{|\mathcal{A}|-1})} \sum_a^{|H_q|} \sum_c^{\mathcal{O}(2^{|\mathcal{A}|-1})} (\delta_b c_a \delta_c^*) P_b P_a P_c. \end{aligned} \quad (\text{B21})$$

We see that the number of terms increases as  $\mathcal{O}(2^{|\mathcal{A}|} |H_q|)$  which was previously shown in [41]. What we show next is additional structure in  $R_S$  - due to the  $X_{kj}$  operators - means the base of the exponent can be slightly lower; however, it still remains exponential in  $|\mathcal{A}|$ .

Consider the adjoint rotation of a particular  $X_{kj}$  in  $R_S$  (Equation B18):

$$\begin{aligned}
R_{S_{kj}} &= \cos\left(\frac{\theta_{kj}}{2}\right)\mathcal{I} + \sin\left(\frac{\theta_{kj}}{2}\right)P_{kj}, \\
R_{S_{kj}}^\dagger &= \cos\left(\frac{\theta_{kj}}{2}\right)\mathcal{I} + \sin\left(\frac{\theta_{kj}}{2}\right)P_{jk}.
\end{aligned} \tag{B22}$$

Performing the adjoint rotation on  $H_q$  results in the following:

$$\begin{aligned}
R_{S_{kj}}H_qR_{S_{kj}}^\dagger &= \left[\alpha_{kj}\mathcal{I} + \beta_{kj}P_{kj}\right] \sum_a c_a P_a \left[\alpha_{kj}\mathcal{I} + \beta_{kj}P_{jk}\right] \\
&= \sum_a c_a (\alpha_{kj}P_a + \beta_{kj}P_{kj}P_a) \left[\alpha_{kj}\mathcal{I} + \beta_{kj}P_{jk}\right] \\
&= \sum_a c_a (\alpha_{kj}^2 P_a + \alpha_{kj}\beta_{kj}P_a P_{jk} + \alpha_{kj}\beta_{kj}\underline{P_{kj}P_a} + \beta_{kj}^2 P_{kj}P_a P_{jk}) \\
&= \sum_a c_a (\alpha_{kj}^2 P_a + \alpha_{kj}\beta_{kj}\underline{P_a P_{jk}} - \alpha_{kj}\beta_{kj}\underline{P_{jk}P_a} + \beta_{kj}^2 P_{kj}P_a P_{jk}) \\
&= \sum_a c_a (\alpha_{kj}^2 P_a + \alpha_{kj}\beta_{kj}[P_a, P_{jk}] + \beta_{kj}^2 P_{kj}P_a P_{jk}) \\
&= \sum_a c_a \begin{cases} (\alpha_{kj}^2 P_a + \beta_{kj}^2 P_{kj}P_a P_{jk}), & \text{if } [P_a, P_{jk}] = 0 \\ (\alpha_{kj}^2 P_a + 2\alpha_{kj}\beta_{kj}P_a P_{jk} + \beta_{kj}^2 P_{kj}P_a P_{jk}), & \text{else } \{P_a, P_{jk}\} = 0 \end{cases}
\end{aligned} \tag{B23}$$

When  $[P_a, P_{jk}] = 0$ , we get:

$$\begin{aligned}
\sum_a c_a (\alpha_{kj}^2 P_a + \beta_{kj}^2 P_{kj}\underline{P_a P_{jk}}) &= \sum_a c_a (\alpha_{kj}^2 P_a + \beta_{kj}^2 \underline{P_{kj}P_a P_{jk}}) \\
&= \sum_a c_a (\alpha_{kj}^2 P_a + \beta_{kj}^2 P_a) \\
&= \sum_a c_a (\alpha_{kj}^2 + \beta_{kj}^2) P_a \\
&= \sum_a c_a P_a.
\end{aligned} \tag{B24}$$

When  $\{P_a, P_{jk}\} = 0$ , we find:

$$\begin{aligned}
\sum_a c_a (\alpha_{kj}^2 P_a + 2\alpha_{kj}\beta_{kj}P_a P_{jk} + \beta_{kj}^2 P_{kj}\underline{P_a P_{jk}}) &= \sum_a c_a (\alpha_{kj}^2 P_a + 2\alpha_{kj}\beta_{kj}P_a P_{jk} - \beta_{kj}^2 \underline{P_{kj}P_a P_{jk}}) \\
&= \sum_a c_a (\alpha_{kj}^2 P_a + 2\alpha_{kj}\beta_{kj}P_a P_{jk} - \beta_{kj}^2 P_a) \\
&= \sum_a c_a (\alpha_{kj}^2 P_a + \sin(\theta_{kj})P_a P_{jk} - \beta_{kj}^2 P_a) \\
&= \sum_a c_a ((\alpha_{kj}^2 - \beta_{kj}^2)P_a + \sin(\theta_{kj})P_a P_{jk}) \\
&= \sum_a c_a (\cos(\theta_{kj})P_a + \sin(\theta_{kj})P_a P_{jk}).
\end{aligned} \tag{B25}$$

Both cases use the following identities:

$$\begin{aligned}
\alpha_{kj}^2 - \beta_{kj}^2 &= \cos^2\left(\frac{\theta_{kj}}{2}\right) - \sin^2\left(\frac{\theta_{kj}}{2}\right) = \cos(\theta_{kj}), \\
\alpha_{kj}^2 + \beta_{kj}^2 &= 1, \\
2\alpha_{kj}\beta_{kj} &= 2\cos\left(\frac{\theta_{kj}}{2}\right)\sin\left(\frac{\theta_{kj}}{2}\right) = \sin(\theta_{kj}),
\end{aligned} \tag{B26}$$

where  $\alpha_{kj} = \cos\left(\frac{\theta_{kj}}{2}\right)$  and  $\beta_{kj} = \sin\left(\frac{\theta_{kj}}{2}\right)$ . Using these results Equation B23 reduces to:

$$\begin{aligned} R_{S_{kj}} H_q R_{S_{kj}}^\dagger &= \sum_{\forall\{P_a, \overset{a}{P}_{jk}\}=0} c_a P_a + \sum_{\forall\{P_a, \overset{a}{P}_{jk}\}=0} c_a \left( \cos(\theta_{kj}) P_a + \sin(\theta_{kj}) P_a P_{jk} \right) \\ &= \sum_a \eta_a P_a + \sum_{\forall\{P_a, \overset{a}{P}_{jk}\}=0} \eta_a (P_{jk} P_a), \end{aligned} \quad (\text{B27})$$

where  $\eta_a$  represent the new real coefficients.

Consider the application of the next rotation operator  $R_{kl}$  in  $R_S$  (note  $k$  index represents the same Pauli operator  $P_k$ ):

$$R_{S_{kl}} R_{S_{kj}} H_q R_{S_{kj}}^\dagger R_{S_{kl}}^\dagger = R_{S_{kl}} \left( \sum_a \eta_a P_a \right) R_{S_{kl}}^\dagger + R_{S_{kl}} \left( \sum_{\forall\{P_a, \overset{a}{P}_{jk}\}=0} \eta_a (P_{jk} P_a) \right) R_{S_{kl}}^\dagger \quad (\text{B28})$$

Focusing on the last term in Equation B28:

$$\begin{aligned} R_{S_{kl}} \left( \sum_{\forall\{P_a, \overset{a}{P}_{jk}\}=0} \eta_a (P_{jk} P_a) \right) R_{S_{kl}}^\dagger &= \left[ \gamma_{kl} \mathcal{I} + \delta_{kl} P_{kl} \right] \sum_{\forall\{P_a, \overset{a}{P}_{jk}\}=0} \eta_a (P_{jk} P_a) \left[ \gamma_{kl} \mathcal{I} + \delta_{kl} P_{lk} \right] \\ &= \sum_{\forall\{P_a, \overset{a}{P}_{jk}\}=0} \eta_a \left( \gamma_{kl} P_{jk} P_a + \delta_{kl} P_{kl} P_{jk} P_a \right) \left[ \gamma_{kl} \mathcal{I} + \delta_{kl} P_{lk} \right] \\ &= \sum_{\forall\{P_a, \overset{a}{P}_{jk}\}=0} \eta_a \left( \gamma_{kl}^2 P_{jk} P_a + \gamma_{kl} \delta_{kl} P_{jk} P_a P_{lk} + \gamma_{kl} \delta_{kl} P_{kl} P_{jk} P_a + \delta_{kl}^2 P_{kl} P_{jk} P_a P_{lk} \right) \\ &= \sum_{\forall\{P_a, \overset{a}{P}_{jk}\}=0} \eta_a \left( \gamma_{kl}^2 P_{jk} P_a + \gamma_{kl} \delta_{kl} P_{jk} P_a P_{lk} - \gamma_{kl} \delta_{kl} P_{kl} P_{jk} P_a + \delta_{kl}^2 P_{kl} P_{jk} P_a P_{lk} \right) \\ &= \sum_{\forall\{P_a, \overset{a}{P}_{jk}\}=0} \eta_a \left( \gamma_{kl}^2 P_{jk} P_a + \gamma_{kl} \delta_{kl} P_{jk} P_a P_{lk} + \gamma_{kl} \delta_{kl} P_{jk} P_{lk} P_a + \delta_{kl}^2 P_{kl} P_{jk} P_a P_{lk} \right) \\ &= \sum_{\forall\{P_a, \overset{a}{P}_{jk}\}=0} \eta_a \left( \gamma_{kl}^2 P_{jk} P_a + \gamma_{kl} \delta_{kl} P_{jk} \{P_a, P_{lk}\} + \delta_{kl}^2 P_{kl} P_{jk} P_a P_{lk} \right) \\ &= \sum_{\forall\{P_a, \overset{a}{P}_{jk}\}=0} \eta_a \begin{cases} \left( \gamma_{kl}^2 P_{jk} P_a + 2\gamma_{kl} \delta_{kl} P_{jk} P_a P_{lk} + \delta_{kl}^2 P_{kl} P_{jk} P_a P_{lk} \right), & \text{if } [P_a, P_{lk}] = 0 \\ \left( \gamma_{kl}^2 P_{jk} P_a + \delta_{kl}^2 P_{kl} P_{jk} P_a P_{lk} \right), & \text{if } \{P_a, P_{lk}\} = 0 \end{cases} \end{aligned} \quad (\text{B29})$$

For the case  $\{P_a, P_{lk}\} = 0$ :

$$\begin{aligned}
\sum_{\forall\{P_a, \overset{a}{P}_{jk}\}=0} \eta_a \left( \gamma_{kl}^2 P_{jk} P_a + \delta_{kl}^2 P_{kl} P_{jk} \underline{P_a P_{lk}} \right) &= \sum_{\forall\{P_a, \overset{a}{P}_{jk}\}=0} \eta_a \left( \gamma_{kl}^2 P_{jk} P_a - \delta_{kl}^2 \underline{P_{kl} P_{jk} P_{lk} P_a} \right) \\
&= \sum_{\forall\{P_a, \overset{a}{P}_{jk}\}=0} \eta_a \left( \gamma_{kl}^2 P_{jk} P_a + \delta_{kl}^2 P_{jk} P_{kl} P_{lk} P_a \right) \\
&= \sum_{\forall\{P_a, \overset{a}{P}_{jk}\}=0} \eta_a \left( \gamma_{kl}^2 P_{jk} P_a + \delta_{kl}^2 P_{jk} P_a \right) \\
&= \sum_{\forall\{P_a, \overset{a}{P}_{jk}\}=0} \eta_a \left( P_{jk} P_a \right).
\end{aligned} \tag{B30}$$

We observe that there is no increase in the number of terms and the weight of each Pauli operator changes.

For the case  $[P_a, P_{lk}] = 0$ :

$$\begin{aligned}
\sum_{\forall\{P_a, \overset{a}{P}_{jk}\}=0} \eta_a \left( \gamma_{kl}^2 P_{jk} P_a + 2\gamma_{kl}\delta_{kl} P_{jk} P_a P_{lk} + \delta_{kl}^2 P_{kl} P_{jk} \underline{P_a P_{lk}} \right) &= \sum_{\forall\{P_a, \overset{a}{P}_{jk}\}=0} \eta_a \left( \gamma_{kl}^2 P_{jk} P_a + 2\gamma_{kl}\delta_{kl} P_{jk} P_a P_{lk} + \delta_{kl}^2 \underline{P_{kl} P_{jk} P_{lk} P_a} \right) \\
&= \sum_{\forall\{P_a, \overset{a}{P}_{jk}\}=0} \eta_a \left( \gamma_{kl}^2 P_{jk} P_a + 2\gamma_{kl}\delta_{kl} P_{jk} P_a P_{lk} - \delta_{kl}^2 P_{jk} P_{kl} P_{lk} P_a \right) \\
&= \sum_{\forall\{P_a, \overset{a}{P}_{jk}\}=0} \eta_a \left( \gamma_{kl}^2 P_{jk} P_a + 2\gamma_{kl}\delta_{kl} P_{jk} P_a P_{lk} - \delta_{kl}^2 P_{jk} P_a \right) \\
&= \sum_{\forall\{P_a, \overset{a}{P}_{jk}\}=0} \eta_a \left( (\gamma_{kl}^2 - \delta_{kl}^2) P_{jk} P_a + 2\gamma_{kl}\delta_{kl} P_{jk} P_a P_{lk} \right) \\
&= \sum_{\forall\{P_a, \overset{a}{P}_{jk}\}=0} \eta_a \left( \cos(\theta_{kl}) P_{jk} P_a + \sin(\theta_{kl}) P_{jk} P_a P_{lk} \right).
\end{aligned} \tag{B31}$$

The number of terms in the resulting operator has increased for each case where  $[P_a, P_{lk}] = 0$ . The action of two rotations of  $R_S$  on the whole Hamiltonian results in:

$$\begin{aligned}
R_{S_{kl}} R_{S_{kj}} H R_{S_{kj}}^\dagger R_{S_{kl}}^\dagger &= R_{S_{kl}} \left( \sum_a \eta_a P_a \right) R_{S_{kl}}^\dagger + R_{S_{kl}} \left( \sum_{\forall\{P_a, \overset{a}{P}_{jk}\}=0} \eta_a (P_{jk} P_a) \right) R_{S_{kl}}^\dagger \\
&= R_{S_{kl}} \left( \sum_a \eta_a P_a \right) R_{S_{kl}}^\dagger + \sum_{\substack{\forall\{P_a, \overset{a}{P}_{jk}\}=0 \\ \forall\{P_a, P_{lk}\}=0}} \eta_a P_{jk} P_a + \\
&\quad \sum_{\substack{\forall\{P_a, \overset{a}{P}_{jk}\}=0 \\ [P_a, P_{lk}]=0}} \eta_a \left( \cos(\theta_{kl}) P_{jk} P_a + \sin(\theta_{kl}) P_{jk} P_a P_{lk} \right) \\
&= R_{S_{kl}} \left( \sum_a \eta_a P_a \right) R_{S_{kl}}^\dagger + \sum_{\forall\{P_a, \overset{a}{P}_{jk}\}=0} \mu_a P_{jk} P_a + \sum_{\substack{\forall\{P_a, \overset{a}{P}_{jk}\}=0 \\ [P_a, P_{lk}]=0}} \mu_a P_{jk} P_a P_{lk} \\
&= \sum_a \nu_a P_a + \sum_{\forall\{P_a, \overset{a}{P}_{lk}\}=0} \nu_a (P_{lk} P_a) + \sum_{\forall\{P_a, \overset{a}{P}_{jk}\}=0} \mu_a P_{jk} P_a + \sum_{\substack{\forall\{P_a, \overset{a}{P}_{jk}\}=0 \\ [P_a, P_{lk}]=0}} \mu_a P_{jk} P_a P_{lk}.
\end{aligned} \tag{B32}$$

where Greek letters are new coefficients according to the expansion. We use the results of Equations B30 and B31 to determine what occurs to the second term of Equation B32. We have applied the result in Equation B27 to the first term  $(R_{S_{kl}} \left( \sum_i \eta_i P_i \right) R_{S_{kl}}^\dagger)$  in Equation B32.

From these results we can infer how the terms in  $H_q$  will scale for a general sequence of rotations of size  $|R_S|$  (Equation B18), which in general change as:

$$|H_q| \sum_{g=0}^{|R_S|} \binom{|R_S|}{g} = 2^{|R_S|} |H_q| \quad (\text{B33})$$

This operation increases the number of terms in  $H_q$  to  $\mathcal{O}(2^{(|A|-1)|H_q|})$ . However, the structure of the sequence of rotation operator actually requires  $2^g$  commuting/anticommuting conditions to be met for new Pauli operators to be generated by subsequent rotations. We therefore need to consider the probability that a given Pauli operator will either commute or anticommute with another. For the case of single qubit Pauli matrices  $\sigma_a, \sigma_b \in \{I, X, Y, Z\}$  by a simple counting argument  $P([\sigma_a, \sigma_b] = 0) = \frac{5}{8}$  and  $P(\{\sigma_a, \sigma_b\} = 0) = \frac{3}{8}$ , for Pauli matrices selected uniformly at random. Generalising this to tensor products of Pauli matrices on  $n$  qubits, for a Pauli operator to anticommute with another there needs to be an odd number of anticommuting tensor factors. First consider the binomial distribution:

$$P(x) = \binom{n}{x} p^x q^{n-x}, \quad (\text{B34})$$

where  $n$  is the number of trials (repeated experiments),  $p$  is the probability of success - here the probability a single Pauli matrix anticommutes with another ( $p = \frac{3}{8}$ ) - and  $q$  is the probability of failure - here the probability a single Pauli matrix commutes with another ( $q = \frac{5}{8}$ ). Under these conditions,  $P(x)$  gives the probability that two  $n$ -fold Pauli operators, selected uniformly at random, anticommute in  $x$ -many tensor factors. Therefore, the probability of two uniformly random Pauli operators anticommuting (commuting) is given as a sum over odd (even) values of  $x \leq n$ :

$$P(\{P_a, P_b\} = 0) = \sum_{c=1}^{\lceil n/2 \rceil} P(2c-1). \quad (\text{B35})$$

Now, the binomial theorem states

$$(p+q)^n = \sum_{c=0}^n \binom{n}{c} p^c q^{n-c} \quad (\text{B36})$$

for any  $p, q \in \mathbb{R}$  and define the following difference:

$$\begin{aligned} (p+q)^n - (-p+q)^n &= \sum_{c=0}^n \binom{n}{c} \underbrace{[1 - (-1)^c]}_{\begin{cases} 2, & \text{if } c \text{ odd} \\ 0, & \text{if } c \text{ even} \end{cases}} p^c q^{n-c} = 2 \sum_{c=1}^{\lceil n/2 \rceil} \binom{n}{2c-1} p^{2c-1} q^{n-(2c-1)}. \end{aligned} \quad (\text{B37})$$

Overall we find the probability that two  $n$ -fold Pauli operators anticommute to be:

$$\begin{aligned} P(\{P_a, P_b\} = 0) &= \sum_{c=1}^{\lceil n/2 \rceil} P(2c-1) \\ &= \sum_{c=1}^{\lceil n/2 \rceil} \binom{n}{2c-1} \cdot \left(\frac{3}{8}\right)^{2c-1} \cdot \left(\frac{5}{8}\right)^{n-(2c-1)} \\ &= \frac{1}{2} \left[ \left(\frac{3}{8} + \frac{5}{8}\right)^n - \left(-\frac{3}{8} + \frac{5}{8}\right)^n \right] \\ &= \frac{1}{2} \left[ 1 - \left(\frac{1}{4}\right)^n \right], \end{aligned} \quad (\text{B38})$$

when each operator  $P_a, P_b$  is chosen uniformly at random. The  $n$  choose  $2c - 1$  term in equation B38 counts all the possible ways an odd number of single qubit pairs of Pauli tensor factors can differ on  $n$  qubits, the first fraction gives the probability that there are  $2c - 1$  anticommuting terms on each pair of qubits and the final fraction gives the probability that the remaining  $n - (2c - 1)$  qubit positions pairwise commute on each qubit. The penultimate line of equation B38 uses the definition in B37, with the factor of two taken into account. Through equation B38, it can be seen that the probability of two  $n$ -fold Pauli operators anticommuting quickly converges to 0.5 as the number of qubits  $n$  increases. The motivation for (B37) arises from observing that the quantity we subtract,  $(1/4)^n$ , is the probability of obtaining an  $n$ -fold identity operator, which has the unique property of commuting universally. The complement  $1 - (1/4)^n$  therefore corresponds with the probability of selecting uniformly at random a Pauli operator with at least one non-trivial tensor factor. After discounting identity operators from consideration, the probabilities of anticommuting or commuting coincide, hence each occurs half of the time, explaining the  $1/2$  factor in (B38); the probability bias towards commutation is a consequence of the identity operator commuting universally, whereas there is no such operator that can anticommute universally.

If we consider how the number of terms in  $H_q$  changes upon the sequence of rotations transformation:  $H_q \mapsto R_S H_q R_S^\dagger$  where terms either commute or anticommute with a probability of 0.5, then the scaling is as follows:

$$\sum_{g=0}^{|R_S|} \frac{|H_q|}{2^g} \binom{|R_S|}{g} = \left(\frac{3}{2}\right)^{|R_S|} |H_q|. \quad (\text{B39})$$

Equation B33 is modified to have a constant factor of  $2^{-g}$ , where  $g$  represents the number of commuting or anticommuting conditions required for operators in  $H_q$  to obey in order to increase the number of terms upon a rotation of  $R_S$ . Here each condition is assumed to occur with a probability of 0.5. This operation increases the number of terms in  $H_q$  to  $\mathcal{O}(1.5^{(|\mathcal{A}|-1)} |H_q|)$ . Note  $|R_S| = |\mathcal{A}| - 1$ . In general, the scaling will be  $\mathcal{O}(x^{(|\mathcal{A}|-1)} |H_q|)$  where  $1 \leq x \leq 2$ , depending on how each rotation in the sequence of rotations commutes with terms in  $H_q$ . The  $x = 1$  case occurs if each rotation in  $R_S$  commutes with the whole Hamiltonian. Apart from this special case, the number of terms in  $H_q$  will increase exponentially with the size of  $\mathcal{A}$  or equivalently with the number of qubits  $n$  (as  $|\mathcal{A}| \leq 2n + 1$  [41]) when  $R$  is defined by a sequence of rotations.

### b. Unitary partitioning via a linear combination of unitaries

Here we show how  $A(\vec{r}) \mapsto P_0^{(k)} = R_{LCU} A(\vec{r}) R_{LCU}^\dagger$ , where  $R_{LCU}$  is defined by a linear combination of Pauli operators. We consider the set of anticommuting Pauli operators making up  $A(\vec{r})$  (Equation 6). We can re-write this Equation, with the term we are reducing to  $(r_k P_0^{(k)})$  outside the sum:

$$A(\vec{r}) = r_k P_0^{(k)} + \sum_{\substack{j=0 \\ \forall j \neq k}}^{N-1} r_j P_0^{(j)}. \quad (\text{B40})$$

To simplify the notation we drop the subscript 0 (denoting the first operator in a clique) and write each  $P_0^{(k)}, P_0^{(j)}$  as  $P_k$  and  $P_j$  respectively.

A re-normalization can be performed on the remaining sum yielding:

$$\begin{aligned} A(\vec{r}) &= r_k P_k + \Omega \sum_{\substack{j=0 \\ \forall j \neq k}}^{N-1} \delta_j P_j \\ &= r_k P_k + \Omega H_{\mathcal{A} \setminus \{r_k P_k\}}, \end{aligned} \quad (\text{B41})$$

where:

$$\sum_{\substack{j=0 \\ \forall j \neq k}}^{N-1} |\delta_j|^2 = 1, \quad (\text{B42a})$$

$$r_j = \Omega \delta_j, \quad (\text{B42b})$$

$$H_{\mathcal{A} \setminus \{r_k P_k\}} = \sum_{\substack{j=0 \\ \forall j \neq k}}^{N-1} \delta_j P_j. \quad (\text{B42c})$$

Using the Pythagorean trigonometric identity:  $\sin^2(x) + \cos^2(x) = 1$ ,  $A(\vec{r})$  can be re-written as:

$$\begin{aligned} A(\vec{r}) &= \cos(\phi_k) P_k + \sin(\phi_k) \sum_{\substack{j=0 \\ \forall j \neq k}}^{N-1} \delta_j P_j \\ &= \cos(\phi_k) P_k + \sin(\phi_k) H_{\mathcal{A} \setminus \{r_k P_k\}}. \end{aligned} \quad (\text{B43})$$

Comparing Equations B41 and B43, it is clear that  $\cos(\phi_k) = r_k$  and  $\sin(\phi_k) = \Omega$ .

It was shown in [15] that one can consider rotations of  $A(\vec{r})$  around an axis that is Hilbert-Schmidt orthogonal to both  $H_{\mathcal{A} \setminus \{r_k P_k\}}$  and  $P_k$ :

$$\mathcal{X} = \frac{i}{2} [H_{\mathcal{A} \setminus \{r_k P_k\}}, P_k] = i \sum_{\substack{j=0 \\ \forall j \neq k}}^{|H_{\mathcal{A} \setminus \{r_k P_k\}}|^{-1}} \delta_j P_j P_k. \quad (\text{B44})$$

$\mathcal{X}$  anticommutes with  $\mathcal{A}$  and is self-inverse [15]:

$$\mathcal{X}^2 = \left( i \sum_{j=0}^{|H_{\mathcal{A} \setminus \{r_k P_k\}}|^{-1}} \delta_j P_j P_k \right) \left( i \sum_{l=0}^{|H_{\mathcal{A} \setminus \{r_k P_k\}}|^{-1}} \delta_l P_l P_k \right), \quad (\text{B45a})$$

$$= - \sum_{j=0}^{|H_{\mathcal{A} \setminus \{r_k P_k\}}|^{-1}} \sum_{l=0}^{|H_{\mathcal{A} \setminus \{r_k P_k\}}|^{-1}} \delta_j \delta_l P_j P_k P_l P_k, \quad (\text{B45b})$$

$$= - \sum_{k=0}^{|H_{\mathcal{A} \setminus \{r_k P_k\}}|^{-1}} \sum_{\substack{l=0 \\ \forall l \neq j}}^{|H_{\mathcal{A} \setminus \{r_k P_k\}}|^{-1}} \delta_j \delta_l P_j P_k P_j P_k - \sum_{j=0}^{|H_{\mathcal{A} \setminus \{r_k P_k\}}|^{-1}} \sum_{\substack{l=0 \\ \forall l \neq j}}^{|H_{\mathcal{A} \setminus \{r_k P_k\}}|^{-1}} \delta_j \delta_l P_j P_k P_l P_k, \quad (\text{B45c})$$

$$= + \sum_{k=0}^{|H_{\mathcal{A} \setminus \{r_k P_k\}}|^{-1}} \delta_j^2 \underbrace{P_k P_j}_{\text{order change}} P_j P_k - \sum_{j=0}^{|H_{\mathcal{A} \setminus \{r_k P_k\}}|^{-1}} \sum_{l>j}^{|H_{\mathcal{A} \setminus \{r_k P_k\}}|^{-1}} \delta_j \delta_l \underbrace{\{P_j P_k, P_l P_k\}}_{=0 \text{ when } j \neq l}, \quad (\text{B45d})$$

$$= + \sum_{j=0}^{|H_{\mathcal{A} \setminus \{r_k P_k\}}|^{-1}} \delta_j^2 \mathcal{I}, \quad (\text{B45e})$$

$$= \mathcal{I} \quad (\text{B45f})$$

and has the following action [15]:

$$\mathcal{X} A(\vec{r}) = i \left( -\sin \phi_k P_k + \cos \phi_k H_{\mathcal{A} \setminus \{r_k P_k\}} \right). \quad (\text{B46})$$

One can also define the rotation [15, 30]:

$$R_{LCU} = e^{(-i\frac{\alpha}{2}\mathcal{X})} = \cos\left(\frac{\alpha}{2}\right)\mathcal{I} - i\sin\left(\frac{\alpha}{2}\right)\mathcal{X} \quad (\text{B47a})$$

$$= \cos\left(\frac{\alpha}{2}\right)\mathcal{I} - i\sin\left(\frac{\alpha}{2}\right)\left(i\sum_{\substack{j=0 \\ \forall j \neq k}}^{|H_{A \setminus \{r_k P_k\}}|-1} \delta_j P_j P_k\right) \quad (\text{B47b})$$

$$= \cos\left(\frac{\alpha}{2}\right)\mathcal{I} + \sin\left(\frac{\alpha}{2}\right)\sum_{\substack{j=0 \\ \forall j \neq k}}^{|H_{A \setminus \{r_k P_k\}}|-1} \delta_j P_j k, \quad (\text{B47c})$$

$$= \delta_{\mathcal{I}}\mathcal{I} + \sum_{\substack{j=0 \\ \forall j \neq k}}^{|H_{A \setminus \{r_k P_k\}}|-1} \delta_j P_j k. \quad (\text{B47d})$$

The conjugate rotation will be:

$$R_{LCU}^\dagger = \cos\left(\frac{\alpha}{2}\right)\mathcal{I} + i\sin\left(\frac{\alpha}{2}\right)i\sum_{\substack{j=0 \\ \forall j \neq k}}^{|H_{A \setminus \{r_k P_k\}}|-1} \delta_j P_j P_k, \quad (\text{B48a})$$

$$= \cos\left(\frac{\alpha}{2}\right)\mathcal{I} + \sin\left(\frac{\alpha}{2}\right)\sum_{\substack{j=0 \\ \forall j \neq k}}^{|H_{A \setminus \{r_k P_k\}}|-1} \delta_j \underbrace{P_k P_j}_{\text{order change}}, \quad (\text{B48b})$$

$$= \delta_{\mathcal{I}}\mathcal{I} + \sum_{\substack{j=0 \\ \forall j \neq k}}^{|H_{A \setminus \{r_k P_k\}}|-1} \delta_j P_k j. \quad (\text{B48c})$$

Note the different order of  $j$  and  $k$  for  $R_{LCU}$  and  $R_{LCU}^\dagger$ . The adjoint action of  $R_{LCU}$  on  $A(\vec{r})$  is:

$$R_{LCU}A(\vec{r})R_{LCU}^\dagger = \cos(\phi_k - \alpha)P_k + \sin(\phi_k - \alpha)H_{A \setminus \{r_k P_k\}}. \quad (\text{B49})$$

By choosing  $\alpha = \phi_k$ , the following transformation occurs  $R_{LCU}A(\vec{r})R_{LCU}^\dagger = P_k$  [15, 30]. This fully defines the  $R_{LCU}$  operator required by unitary partitioning. Next we need to consider the use of this operator in CS-VQE.

The adjoint action of  $R_{LCU}$  on a general Hamiltonian  $H_q = \sum_i^{|H_q|} c_i P_i$  is:

$$R_{LCU}H_qR_{LCU}^\dagger = \left(\delta_{\mathcal{I}}\mathcal{I} + \sum_j^{|R_{LCU}|-1} \delta_j P_j k\right) \sum_i^{|H_q|} c_i P_i \left(\delta_{\mathcal{I}}\mathcal{I} + \sum_l^{|R_{LCU}|-1} \delta_l P_{kl}\right) \quad (\text{B50a})$$

$$= \left(\delta_{\mathcal{I}} \sum_i^{|H_q|} c_i P_i + \sum_j^{|R_{LCU}|-1} \sum_i^{|H_q|} \delta_j c_i P_j k P_i\right) \left(\delta_{\mathcal{I}}\mathcal{I} + \sum_l^{|R_{LCU}|-1} \delta_l P_{kl}\right) \quad (\text{B50b})$$

$$= \delta_{\mathcal{I}}^2 \sum_i^{|H_q|} c_i P_i \quad (\text{B50c})$$

$$+ \sum_l^{|R_{LCU}|-1} \sum_i^{|H_q|} \delta_{\mathcal{I}} c_i \delta_l P_i P_{kl} + \sum_j^{|R_{LCU}|-1} \sum_i^{|H_q|} \delta_{\mathcal{I}} \delta_j c_i P_j k P_i \quad (\text{B50d})$$

$$+ \sum_j^{|R_{LCU}|-1} \sum_i^{|H_q|} \sum_l^{|R_{LCU}|-1} \delta_j c_i \delta_l P_j k P_i P_{kl} \quad (\text{B50e})$$

We can rewrite the final term (Equation B50e) as:

$$\sum_j^{|R_{LCU}|-1} \sum_i^{|H_q|} \sum_l^{|R_{LCU}|-1} \delta_j c_i \delta_l P_{jk} P_i P_{kl} = \sum_j^{|R_{LCU}|-1} \sum_i^{|H_q|} \sum_{\substack{l=j \\ [P_{jk}, P_i]=0}}^{|R_{LCU}|-1} (c_i \delta_j \delta_j^*) P_i \quad (\text{B51a})$$

$$+ \sum_j^{|R_{LCU}|-1} \sum_i^{|H_q|} \sum_{\substack{l=j \\ \{P_{jk}, P_i\}=0}}^{|R_{LCU}|-1} (-c_i \delta_j \delta_j^*) P_i \quad (\text{B51b})$$

$$+ \sum_j^{|R_{LCU}|-1} \sum_i^{|H_q|} \sum_{l \neq j}^{|R_{LCU}|-1} (\delta_j c_i \delta_l) P_{jk} P_i P_{kl}. \quad (\text{B51c})$$

Here we have applied the identity of conjugating a Pauli operator  $P_u$  with another Pauli operator  $P_v$  resulting in two cases:

$$P_v P_u P_v = \begin{cases} P_u, & \text{if } [P_v, P_u] = 0 \\ -P_u, & \text{otherwise } \{P_v, P_u\} = 0 \end{cases} \quad (\text{B52})$$

Focusing on the last term of Equation B51, we can simplify B51c as  $j$  and  $l$  run over the same indices we can re-write each  $l \neq j$  sum as  $l > j$  and expand into two terms:

$$\sum_j^{|R_{LCU}|-1} \sum_i^{|H_q|} \sum_{l \neq j}^{|R_{LCU}|-1} (\delta_j c_i \delta_l) P_{jk} P_i P_{kl} = \sum_j^{|R_{LCU}|-1} \sum_i^{|H_q|} \sum_{l > j}^{|R_{LCU}|-1} (\delta_j c_i \delta_l) (P_{jk} P_i P_{kl} + P_{lk} P_i P_{kj}) \quad (\text{B53})$$

We can expand then expand this equation into the four cases for when:

1.  $[P_{jk}, P_i] = 0$  and  $[P_{lk}, P_i] = 0$
2.  $[P_{jk}, P_i] = 0$  and  $\{P_{lk}, P_i\} = 0$
3.  $\{P_{jk}, P_i\} = 0$  and  $[P_{lk}, P_i] = 0$
4.  $\{P_{jk}, P_i\} = 0$  and  $\{P_{lk}, P_i\} = 0$

For the first case and last case:

$$\begin{aligned} \sum_j^{|R_{LCU}|-1} \sum_i^{|H_q|} \sum_{l > j}^{|R_{LCU}|-1} (\delta_j c_i \delta_l) (P_{jk} P_i P_{kl} + P_{lk} P_i P_{kj}) &= \sum_j^{|H_q|} \sum_i^{|H_q|} \sum_{l > j}^{|H_q|} (\delta_j c_i \delta_l) (\pm P_i P_{jk} P_{kl} \pm P_i P_{lk} P_{kj}) \\ &= \sum_j^{|H_q|} \sum_i^{|H_q|} \sum_{l > j}^{|H_q|} (\delta_j c_i \delta_l) (\pm P_i P_j P_l \pm P_i P_l P_j) \\ &= \sum_j^{|H_q|} \sum_i^{|H_q|} \sum_{l > j}^{|H_q|} (\delta_j c_i \delta_l) \pm P_i \{P_j, P_l\} \\ &= 0 \end{aligned} \quad (\text{B54})$$

Whereas, for the second and third cases:

$$\begin{aligned}
\sum_j^{|R_{LCU}|-1} \sum_i^{|H_q|} \sum_{l>j}^{|R_{LCU}|-1} (\delta_j c_i \delta_l) \left( \underline{P_{jk} P_i P_{kl}} + \underline{P_{lk} P_i P_{kj}} \right) &= \sum_j \sum_i^{|H_q|} \sum_{l>j} (\delta_j c_i \delta_l) \left( \pm P_i \underline{P_{jk} P_{kl}} \mp P_i \underline{P_{lk} P_{kj}} \right) \\
&= \sum_j \sum_i^{|H_q|} \sum_{l>j} (\delta_j c_i \delta_l) \left( \pm P_i P_j P_l \mp P_i P_l P_j \right) \\
&= \sum_j \sum_i^{|H_q|} \sum_{l>j} (\delta_j c_i \delta_l) \left( \pm P_i P_j P_l \pm P_i P_j P_l \right) \\
&= \sum_j \sum_i^{|H_q|} \sum_{l>j} (\delta_j c_i \delta_l) \pm 2 P_i P_j P_l
\end{aligned} \tag{B55}$$

We can rewrite Equation B51 using this result:

$$\begin{aligned}
\sum_j^{|R_{LCU}|-1} \sum_i^{|H_q|} \sum_l^{|R_{LCU}|-1} \delta_j c_i \delta_l P_{jk} P_i P_{kl} &= \sum_j \sum_i^{|H_q|} \sum_{\substack{l=j \\ [P_{jk}, P_i]=0}} (c_i \delta_j \delta_j^*) P_i + \sum_j \sum_i^{|H_q|} \sum_{\substack{l=j \\ \{P_{jk}, P_i\}=0}} (-c_i \delta_j \delta_j^*) P_i + \\
&\quad \sum_j \sum_i^{|H_q|} \sum_{\substack{l>j \\ \forall [P_{jk}, P_i]=0 \\ \{P_{jk}, P_i\}=0}} (\delta_j c_i \delta_l) 2 P_i P_j P_l - \sum_j \sum_i^{|H_q|} \sum_{\substack{l>j \\ \forall \{P_{jk}, P_i\}=0 \\ [P_{lk}, P_i]=0}} (\delta_j c_i \delta_l) 2 P_i P_j P_l \\
&= \sum_i^{|H_q|} \nu_i P_i + \sum_j^{|R_{LCU}|-1} \sum_i^{|H_q|} \sum_{\substack{l>j \\ \forall \{P_i, P_j P_l\}=0}}^{|R_{LCU}|-1} \nu_{ijl} P_i P_j P_l
\end{aligned} \tag{B56}$$

where we have combined the second and third conditions into a single condition of  $\{P_a, P_{jk} P_{kl}\} = \{P_a, P_j P_l\} = 0$  and combined the new coefficients into one coefficient denoted  $\nu$ .

Next consider the B50d term of equation B50. One can use the fact that  $j$  and  $l$  run over the same indices:

$$\begin{aligned}
\underbrace{\sum_l^{|R_{LCU}|-1} \sum_i^{|H_q|} \delta_{\mathcal{I}} c_i \delta_l P_i P_{kl}}_{\text{re-write using } l=j} + \sum_j^{|R_{LCU}|-1} \sum_i^{|H_q|} \delta_{\mathcal{I}} \delta_j c_i P_{jk} P_i &= \sum_j^{|R_{LCU}|-1} \sum_i^{|H_q|} \delta_{\mathcal{I}} c_i \delta_j P_i P_{kj} + \sum_j^{|R_{LCU}|-1} \sum_i^{|H_q|} \delta_{\mathcal{I}} \delta_j c_i P_{jk} P_i \\
&= \sum_j^{|R_{LCU}|-1} \sum_i^{|H_q|} -\delta_{\mathcal{I}} c_i \delta_j P_i P_{jk} + \sum_j^{|R_{LCU}|-1} \sum_i^{|H_q|} \delta_{\mathcal{I}} \delta_j c_i P_{jk} P_i \\
&= \sum_j^{|R_{LCU}|-1} \sum_i^{|H_q|} \delta_{\mathcal{I}} c_i \delta_j (P_{jk} P_i - P_i P_{jk}) \\
&= \sum_j^{|R_{LCU}|-1} \sum_i^{|H_q|} \delta_{\mathcal{I}} c_i \delta_j [P_{jk}, P_i] \\
&= \sum_j^{|R_{LCU}|-1} \sum_{\substack{i \\ \forall \{P_{jk}, P_i\}=0}}^{|H_q|} 2 \delta_{\mathcal{I}} c_i \delta_j P_{jk} P_i
\end{aligned} \tag{B57}$$

Overall we can re-write equation B50 using the result of B56 and B57 yielding:

$$\begin{aligned}
R_{LCU}H_qR_{LCU}^\dagger &= \underbrace{\delta_{\mathcal{I}}^2 \sum_i^{|H_q|} c_i P_i}_{B50c} + \underbrace{\sum_j^{|R_{LCU}|-1} \sum_{\substack{i \\ \forall \{P_{jk}, P_i\}=0}}^{|H_q|} 2\delta_{\mathcal{I}} c_i \delta_j P_{jk} P_i}_{B50d} + \\
&\underbrace{\sum_i^{|H_q|} \nu_i P_i + \sum_j^{|R_{LCU}|-1} \sum_i^{|H_q|} \sum_{\substack{l>j \\ \forall \{P_i, P_j, P_l\}=0}}^{|R_{LCU}|-1} \nu_{ijl} P_i P_j P_l}_{B50e} \\
&= \delta_{\mathcal{I}}^2 \sum_i^{|H_q|} (c_i + \nu_i) P_i + \sum_j^{|R_{LCU}|-1} \sum_{\substack{i \\ \forall \{P_{jk}, P_i\}=0}}^{|H_q|} 2\delta_{\mathcal{I}} c_i \delta_j P_{jk} P_i + \\
&\sum_j^{|R_{LCU}|-1} \sum_i^{|H_q|} \sum_{\substack{l>j \\ \forall \{P_i, P_j, P_l\}=0}}^{|R_{LCU}|-1} \nu_{ijl} P_i P_j P_l
\end{aligned} \tag{B58}$$

We observe that the number of terms in  $R_{LCU}H_qR_{LCU}^\dagger$  at worst scales as  $|H_q| + |H_q| \cdot (|R_{LCU}| - 1) + |H_q| \left( \frac{(|R_{LCU}|-1)(|R_{LCU}|-2)}{2} \right)$  or  $\mathcal{O}(|H_q| \cdot |\mathcal{A}|^2)$ . The total number of qubits  $n$  bounds the size of  $|\mathcal{A}| \leq 2n + 1$  [41], and thus the number of terms in  $H_q$  will increase quadratically with the size of  $\mathcal{A}$  or number of qubits  $n$  when  $R$  is defined by a linear combination of unitaries.

### c. Mapping Pauli operators to single-qubit Pauli Z operators

In Appendix A of [14] a proof is given on how to map a completely commuting set of Pauli operators to a single qubit Pauli Z operator. We summarise the operation required and omit the proof. We denote a given Pauli operator on  $n$  qubits as:  $P = \bigotimes_{i=0}^{n-1} \sigma_i^{P_i}$ , where  $\sigma_i$  are a single qubit Pauli operators. There are two cases we need to consider (diagonal and non-diagonal), with the goal to reduce the operators in  $\mathcal{R}' \equiv \{P_0^{(k)}\} \cup \mathcal{G}$  (Equation 8) to single-qubit Z Pauli operators.

For a non-diagonal Pauli operators  $P_a \in \mathcal{R}'$ , there must be at least one single qubit Pauli operator indexed by qubit  $k$  such that:  $\sigma_k^{P_a} \in \{X, Y\}$ . We can use this to define operator  $P_b$  that must anticommute with  $P_a$ :

$$\begin{aligned}
P_a &= \left( \bigotimes_{i=0}^{k-1} \sigma_i^{P_a} \right) \otimes \sigma_k^{P_a} \otimes \left( \bigotimes_{i=k+1}^{n-1} \sigma_i^{P_a} \right) \\
P_b &= \left( \bigotimes_{i=0}^{k-1} \sigma_i^{P_a} \right) \otimes \sigma_k' \otimes \left( \bigotimes_{i=k+1}^{n-1} \sigma_i^{P_a} \right)
\end{aligned} \quad \text{where } \{P_a, P_b\} = 0 \Leftrightarrow \sigma_k' = \begin{cases} X, & \text{if } \sigma_k^{P_a} = Y \\ Y, & \text{if } \sigma_k^{P_a} = X \end{cases} \tag{B59}$$

These two Pauli operators differ by exactly one Pauli operator on qubit index  $k$ . We can define the rotation:

$$B = \exp\left(i\frac{\pi}{4}P_b\right) \tag{B60}$$

Conjugating  $P_a$  with this operator results in:

$$BP_aB^\dagger = \pm 1 \left( \bigotimes_{i=0}^{k-1} I_i \right) \otimes Z_k \otimes \left( \bigotimes_{i=k+1}^{n-1} I_i \right) = P'_a, \tag{B61}$$

and  $P_a$  has been mapped to a single qubit Pauli Z operator.

For diagonal operators  $P_c \in \mathcal{R}'$ , all the  $n$ -fold tensor products of single qubit Pauli operators must be either Z or I:  $P_c = \bigotimes_{i=0}^{n-1} \sigma_i^{P_c}$  where  $\sigma_i^{P_c} \in \{I, Z\} \forall i$ . Since  $\mathcal{R}'$  is an independent set, for all the rotated  $P'_a$  there must be at

least one index  $l$  such that  $\sigma_l^{P'_a} = I$  and  $\sigma_l^{P_c} = Z$ . We denote this operator  $P_c$ . We also define a new operator  $P_d$  from this, which only acts non-trivially on the  $l$ -th qubit with a single qubit  $Y$ . To summarise:

$$\begin{aligned}
P_c &= \left( \bigotimes_{i=0}^{l-1} \sigma_i^{P'_c} \right) \otimes Z_l \otimes \left( \bigotimes_{i=l+1}^{n-1} \sigma_i^{P'_c} \right) \text{ where } \sigma_i^{P'_c} \in \{I, Z\} \forall i \\
P_d &= \left( \bigotimes_{i=0}^{l-1} I_i \right) \otimes Y_l \otimes \left( \bigotimes_{i=l+1}^{n-1} I_i \right) \\
P'_a &= \left( \bigotimes_{i=0}^{l-1} \sigma_i^{P'_a} \right) \otimes I_l \otimes \left( \bigotimes_{i=l+1}^{n-1} \sigma_i^{P'_a} \right) \text{ where } [P_d, P'_a] = 0 \text{ and } \sigma_i^{P'_a} \in \{I, Z\} \forall i
\end{aligned} \tag{B62}$$

We can define the rotation:

$$D = \exp\left(i \frac{\pi}{4} P_d\right) \tag{B63}$$

Conjugating  $P_c$  with this operator results in:

$$DP_c D^\dagger = \pm 1 \left( \bigotimes_{i=0}^{l-1} \sigma_i^{P'_c} \right) \otimes X_l \otimes \left( \bigotimes_{i=l+1}^{n-1} \sigma_i^{P'_c} \right) = P'_c. \tag{B64}$$

$P'_c$  is now a non-diagonal Pauli operator (contains a single qubit  $X$  acting on qubit  $l$ ). This operator  $P'_c$  can now be mapped to a single qubit  $Z$  operator using a further  $\frac{\pi}{2}$ -rotation following the previously given procedure for diagonal Pauli operators.

The operators  $V_i$  in the main text (equation 11) are defined by these  $\frac{\pi}{2}$ -rotations, such that each  $q_i G_i$  and  $P_0^{(k)}$  is mapped to a single qubit Pauli  $Z$  term. At worst, two  $\frac{\pi}{2}$ -rotations are needed for every operator in  $\mathcal{R}'$  (Equation 8), which occurs when all operators in  $\mathcal{R}'$  are diagonal.

### Appendix C: Numerical details of the toy example

This section provides all the details for the Toy problem described in Section III B. The full noncontextual ground state is:

$$\underbrace{(-1, +1, -1)}_{\vec{q}_0}, \underbrace{(0.25318483, -0.65828059, -0.70891756)}_{\vec{r}_0}. \tag{C1}$$

This defines the  $A(\vec{r}_0)$ :

$$A(\vec{r}_0) = 0.25318483 YXYI - 0.65828059 XYXI - 0.70891756 XZ XI. \tag{C2}$$

The operators to map  $A(\vec{r}_0)$  to a single Pauli operator are:

$$R_S = e^{+1i \cdot -0.7879622757719398 \cdot ZYZI} \cdot e^{+1i \cdot 1.2036225088338255 \cdot ZZZI}, \tag{C3}$$

and

$$R_{LCU} = 0.79157591 IIII + 0.41580383i ZZZI - 0.44778874i ZYZI. \tag{C4}$$

Their action results in:  $R_S A(\vec{r}_0) R_S^\dagger = R_{LCU} A(\vec{r}_0) R_{LCU}^\dagger = YXYI$ .

We then defined  $U$  depending on which generators we wish to fix. We found the optimal ordering of stabilizers (supplied in Equation 25) to fix via a brute force search. The following order was obtained:

$W$	$U_{\mathcal{W}}^\dagger$	$W^Z = U_{\mathcal{W}}^\dagger W U_{\mathcal{W}}$	$Q_{\mathcal{W}}$	$Q_{\mathcal{W}}^\dagger U_{\mathcal{W}}^\dagger H U_{\mathcal{W}} Q_{\mathcal{W}}$
-1 YIYI		- ZIII		
+1 IXYI	$e^{i\frac{\pi}{2}XYI} e^{i\frac{\pi}{2}IYYI} R_{S/LCU}$	+ IZII	$ 1\rangle\langle 1  \otimes  0\rangle\langle 0  \otimes  1\rangle\langle 1  \otimes  0\rangle\langle 0 $	-2.475+0.000j
-1 IIIZ		- IIIZ		
$\mathcal{A}(\vec{r}_0)$		+ IIZI		
+1 IXYI		+ IZII		
-1 IIIZ	$e^{i\frac{\pi}{2}IYYI} R_{S/LCU}$	- IIIZ	$I \otimes  0\rangle\langle 0  \otimes  0\rangle\langle 0  \otimes  1\rangle\langle 1 $	SeqRot -1.827+0.000j I + -0.198+0.000j X + -0.467+0.000j Z + 0.648+0.000j Y
$\mathcal{A}(\vec{r}_0)$		+ IIZI		LCU -1.827+0.000j I + -0.414+0.000j X + -0.292+0.000j Z + 0.648+0.000j Y
+1 IXYI		+ IZII		
-1 IIIZ	$e^{i\frac{\pi}{2}IYYI}$	- IIIZ	$I \otimes  0\rangle\langle 0  \otimes I \otimes  1\rangle\langle 1 $	-0.500+0.000j II + 0.500+0.000j XI + 0.700+0.000j XX + 0.100+0.000j YI + -0.100+0.000j YX + 1.300+0.000j XZ + 0.600+0.000j IY + 0.700+0.000j ZZ
-1 IIIZ	$IIII$	-IIIZ	$I \otimes I \otimes I \otimes  1\rangle\langle 1 $	-0.500+0.000j III + 0.100+0.000j XXX + 0.200+0.000j YXX + 0.700+0.000j XZX + 0.700+0.000j XYX + 0.100+0.000j YZX + 0.200+0.000j XXZ + 0.600+0.000j IYY + 0.500+0.000j XXY + 0.100+0.000j YXY + 0.600+0.000j XZZ + 0.700+0.000j ZZZ + 0.200+0.000j YYZ + 0.100+0.000j ZYY

TABLE IV: Different contextual subspace Hamiltonians defined from  $H$  (Equation 16).  $R_S$  and  $R_{LCU}$  are defined in Equations C3 and C4.

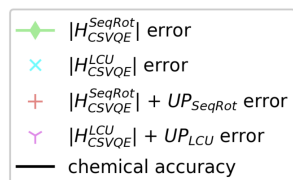
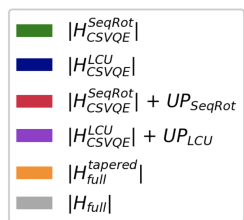
1.  $\{-1 IIIZ\}$
2.  $\{+1 IXYI, -1 IIIZ, \}$
3.  $\{+1 IXYI, -1 IIIZ, +1 \mathcal{A}(\vec{r}_0)\}$
4.  $\{-1 YIYI, +1 IXYI, -1 IIIZ, +1 \mathcal{A}(\vec{r}_0)\}$ .

This defines all the information required to implement CS-VQE. Table IV summarises the stabilizers fixed, the rotation  $U_{\mathcal{W}}$ , required projection  $Q_{\mathcal{W}}$  and final projected Hamiltonian  $Q_{\mathcal{W}}^\dagger U_{\mathcal{W}}^\dagger H U_{\mathcal{W}} Q_{\mathcal{W}}$  for this ordering.

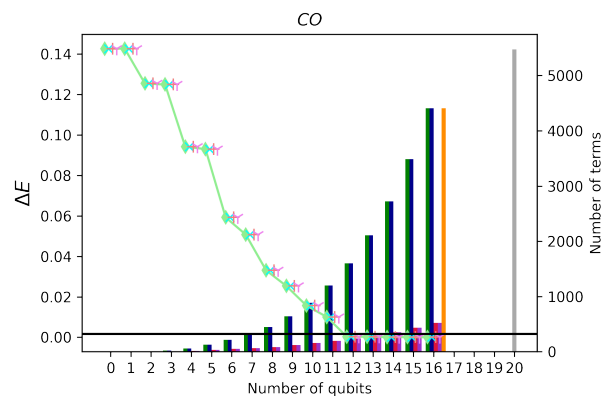
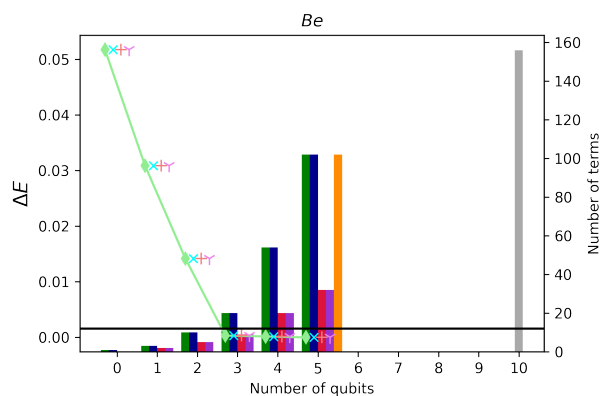
The old approach of applying  $U_{\mathcal{W}_{all}}^\dagger H U_{\mathcal{W}_{all}}$  and then fixing certain stabilizer eigenvalues are summarised in Table V. It can be seen from these results, that always implementing the unitary partitioning rotation  $R$  can unnecessarily increase the number of terms in the Hamiltonian and thus should only be applied if the eigenvalue for  $\langle A(\vec{r}) \rangle$  is fixed.



## Appendix D: Graphical Results for CS-VQE simulation of each Molecular Hamiltonian

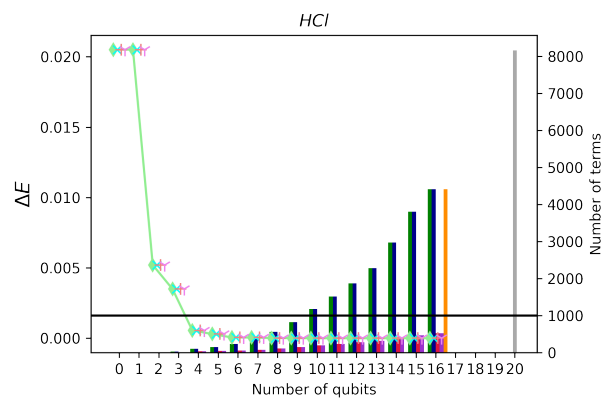
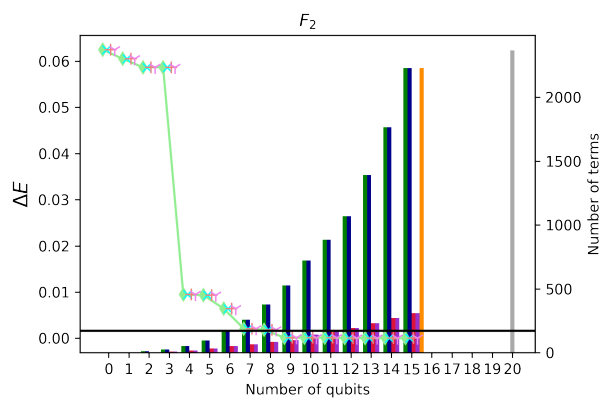


(a)



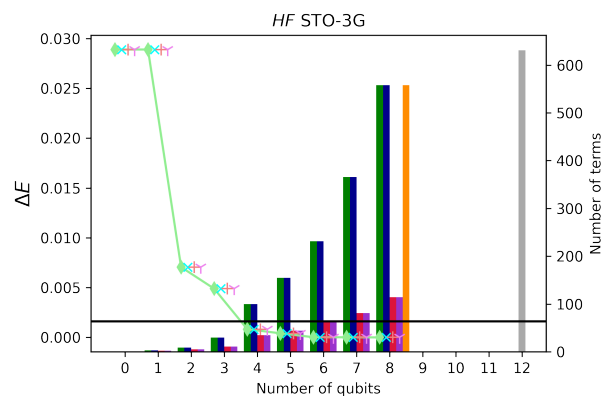
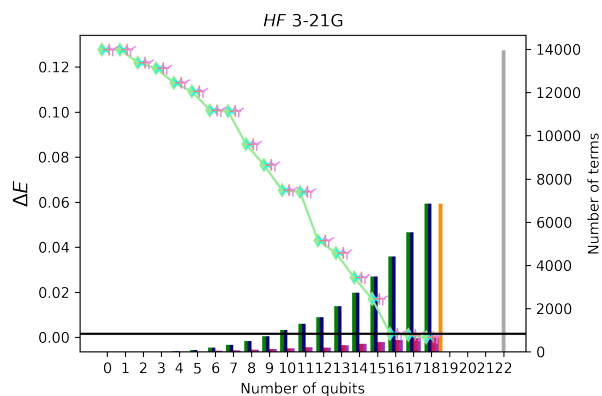
(b)

(c)



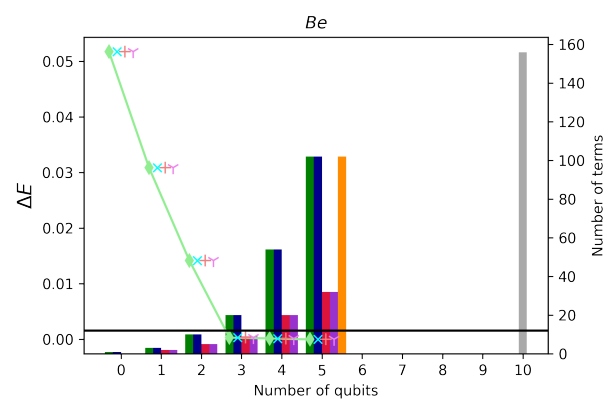
(d)

(e)

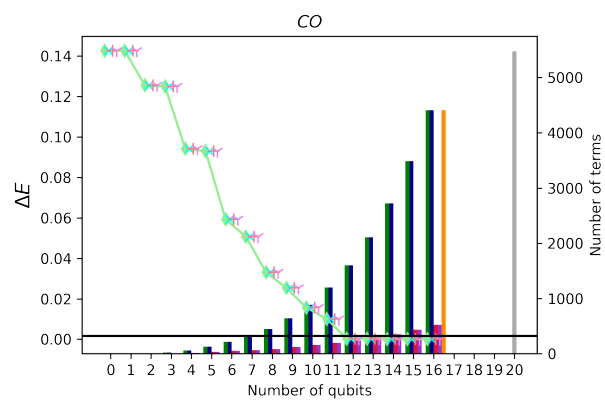


(f)

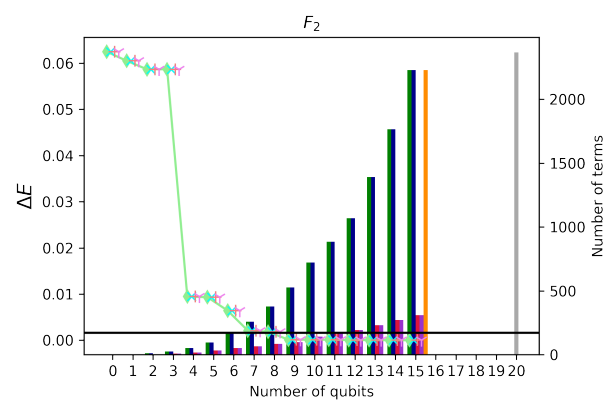
(g)



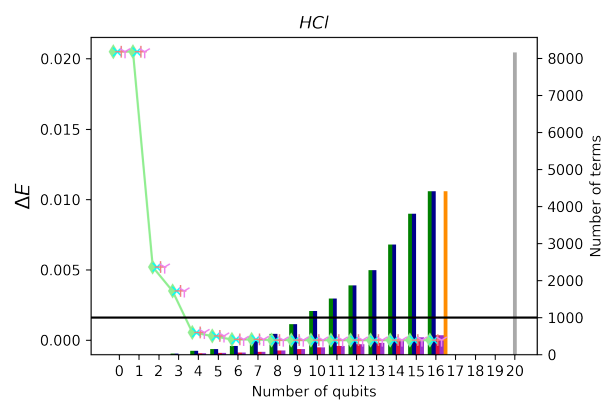
(h)



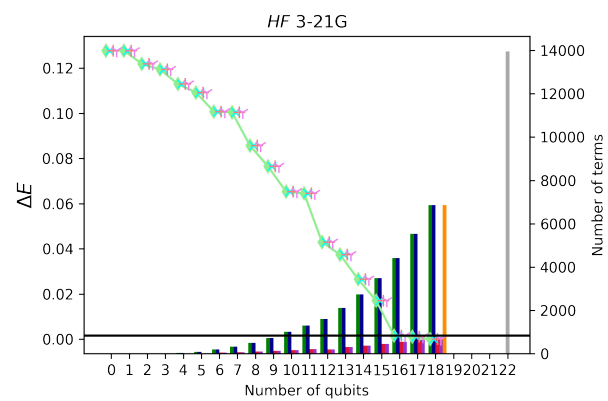
(i)



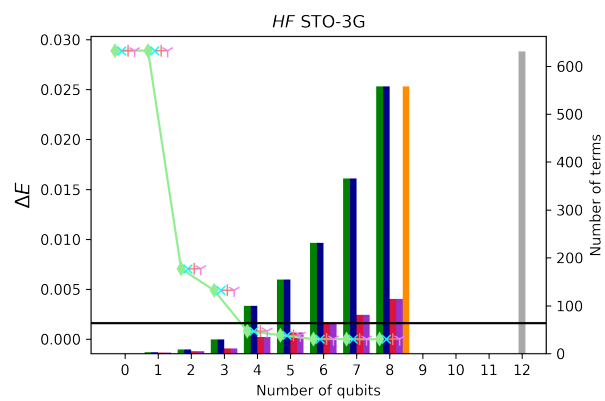
(j)



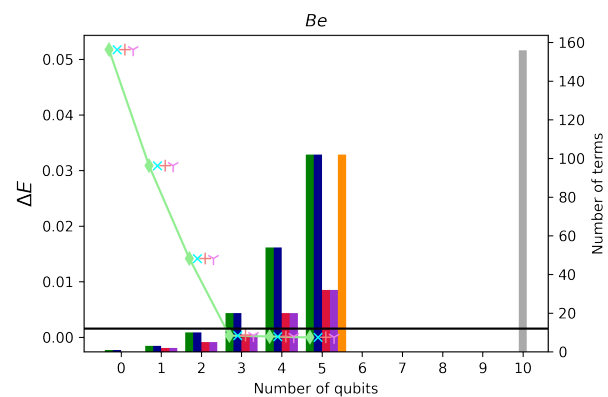
(k)



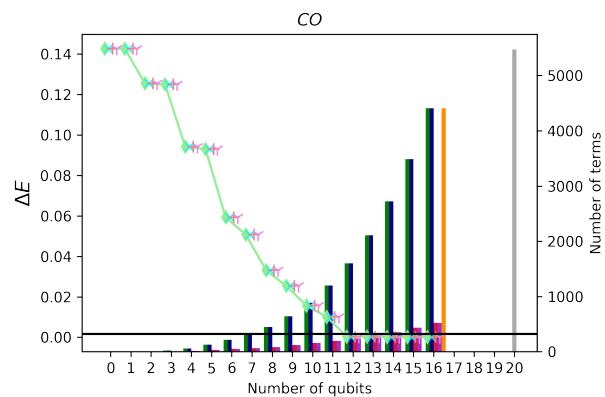
(l)



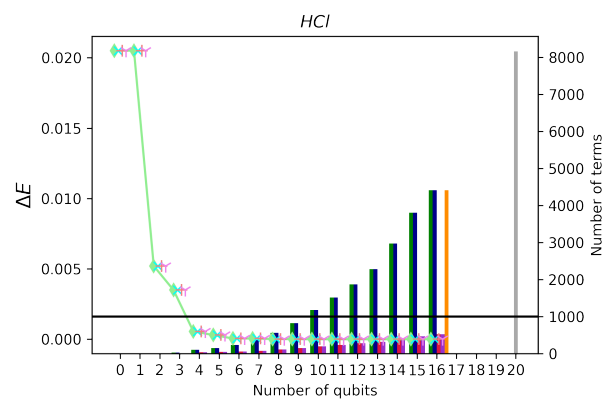
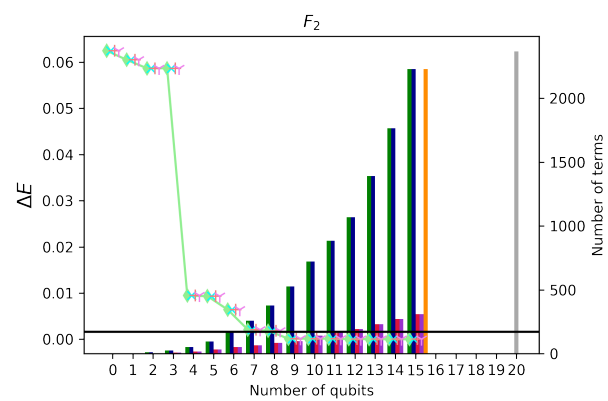
(m)



(n)

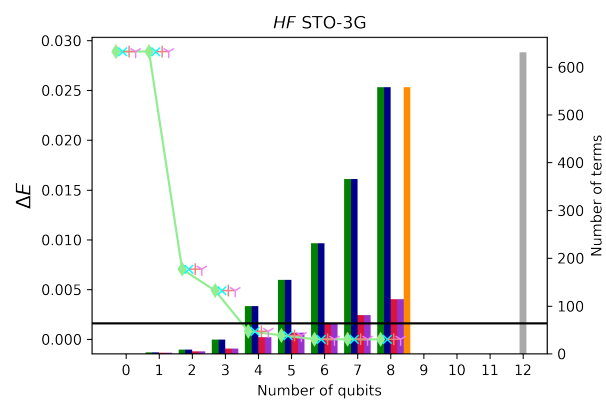
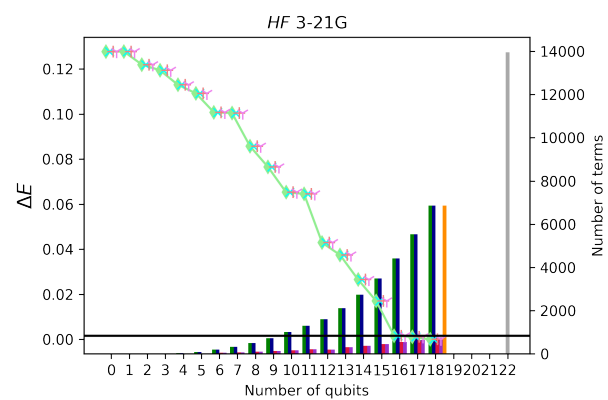


(o)



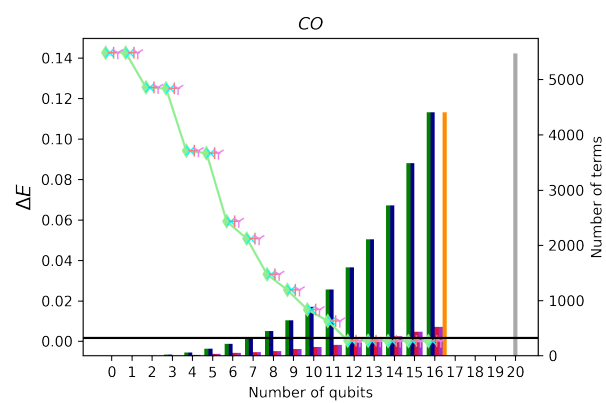
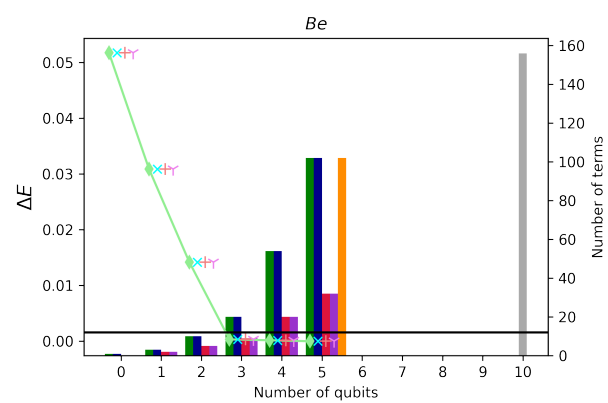
(p)

(q)



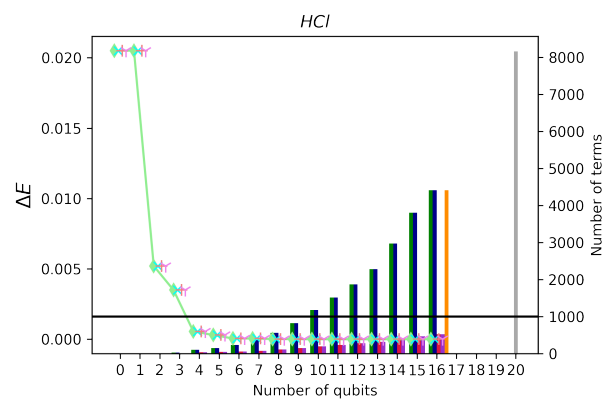
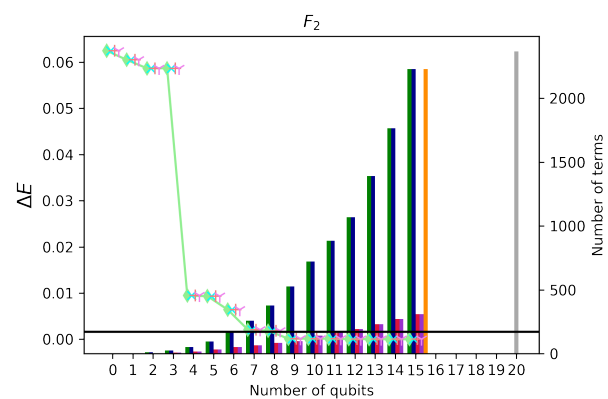
(r)

(s)



(t)

(u)



(v)

(w)

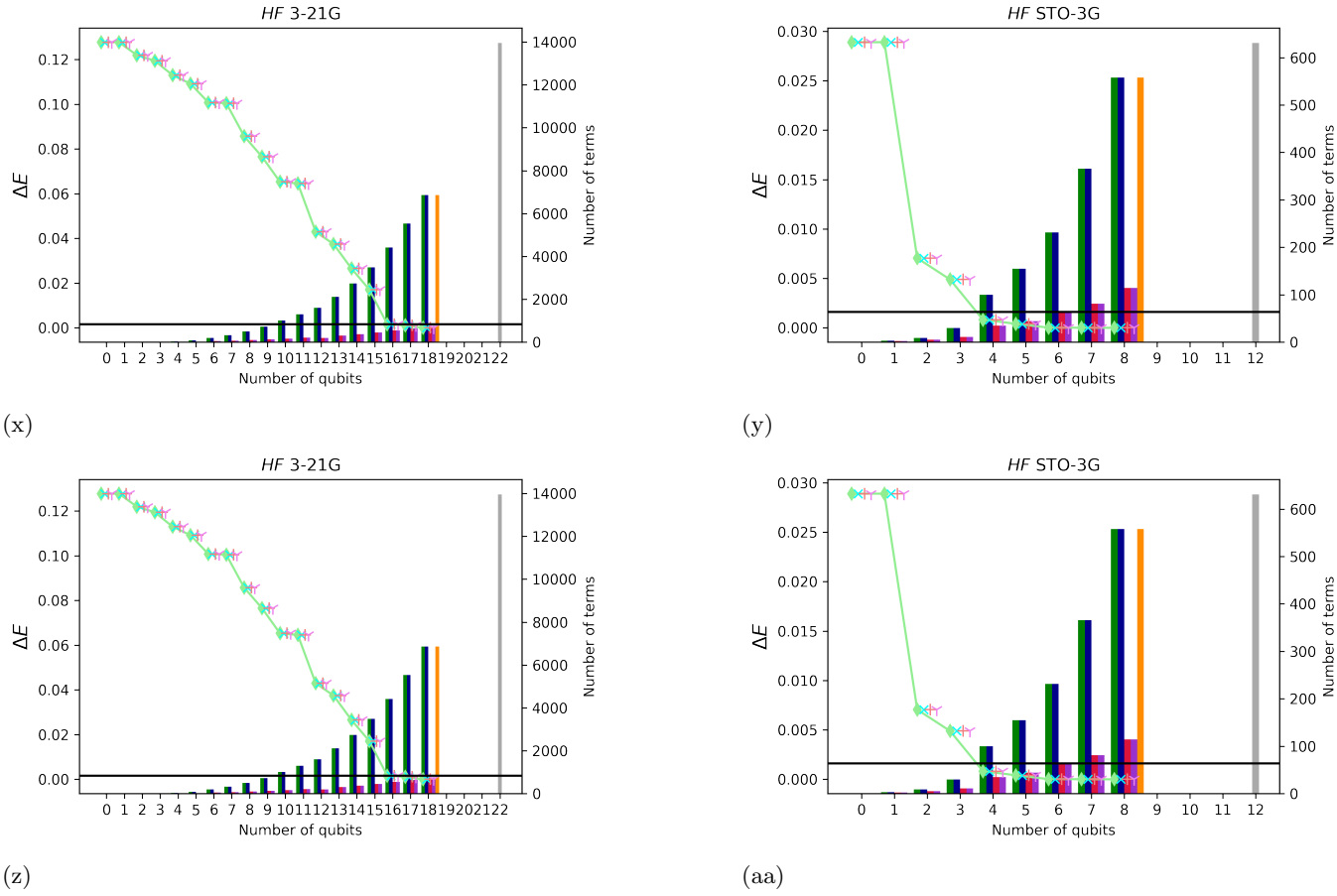


FIG. 4: CS-VQE approximation errors  $\Delta E$  versus number of qubits used on the quantum computer (scatter plot). The horizontal solid black lines indicate chemical accuracy. The number of terms in each Hamiltonian is given by the bar chart.

All the subplots in Figure 4 give the simulation results of each molecular Hamiltonian at different levels of non-contextual approximations. This is equivalent to how many contextual stabilizers  $\mathcal{W}$  eigenvalues are fixed. In each plot, the leftmost data represents the case when all the noncontextual stabilizer eigenvalues are fixed and is the case for the full noncontextual approximation to a given problem [41]. Moving right, we remove a single stabilizer from  $\mathcal{W}$  and thus don't fix the eigenvalue of that stabilizer. This reintroduces a qubits worth degree of freedom into the problem. At the limit that no stabilizer eigenvalues are fixed ( $\mathcal{W} = \{\}$ ) we return to standard VQE over the full problem and no noncontextual approximation is made. In each plot this scenario is represented by the far right data point (excluding the data for the full non tapered Hamiltonian that is supplied for reference only). The raw data for these results is supplied in ancillary files hosted on arXiv.

**Appendix E: Tabulated Results of simulation**

Table VI summarises the numerical results of Figures 2 and 3.

molecule	basis	$H_{\text{CS-VQE}}$	$H_{\text{CS-VQE}} + UP^{(LCU)}$	$H_{\text{CS-VQE}} + UP^{(SeqRot)}$	$H_{\text{tapered}}$	$RH_{\text{tapered}}R^\dagger$	$H_{\text{full}}$
BeH <sub>2</sub>	STO-3G	(7, 268)	(7, 61)	(7, 61)	(9, 596)	(9, 614)	(14, 666)
Mg	STO-3G	(10, 675)	(10, 114)	(10, 114)	(13, 1465)	(13, 1465)	(18, 3388)
H <sub>3</sub> <sup>+</sup>	3-21G	(9, 914)	(9, 115)	(9, 115)	(9, 914)	(9, 786)	(12, 1501)
O <sub>2</sub>	STO-3G	(11, 815)	(11, 157)	(11, 157)	(15, 2229)	(15, 2374)	(20, 2255)
OH	STO-3G	(6, 231)	(6, 62)	(6, 62)	(8, 558)	(8, 558)	(12, 631)
CH <sub>4</sub>	STO-3G	(12, 1359)	(12, 203)	(12, 203)	(14, 2194)	(14, 2194)	(18, 5288)
Be	STO-3G	(3, 20)	(3, 9)	(3, 9)	(5, 102)	(5, 108)	(10, 156)
NH <sub>3</sub>	STO-3G	(11, 1733)	(11, 200)	(11, 200)	(13, 3048)	(13, 2738)	(16, 4293)
H <sub>2</sub> S	STO-3G	(7, 435)	(7, 92)	(7, 92)	(18, 6237)	(18, 6237)	(22, 6246)
H <sub>2</sub>	3-21G	(5, 122)	(5, 27)	(5, 27)	(5, 122)	(5, 124)	(8, 185)
HF	3-21G	(17, 5530)	(17, 648)	(17, 648)	(18, 6852)	(18, 6852)	(22, 13958)
F <sub>2</sub>	STO-3G	(9, 527)	(9, 99)	(9, 99)	(15, 2229)	(15, 2229)	(20, 2367)
HCl	STO-3G	(4, 100)	(4, 35)	(4, 35)	(16, 4409)	(16, 4409)	(20, 8159)
HeH <sup>+</sup>	3-21G	(5, 155)	(5, 35)	(5, 35)	(6, 319)	(6, 319)	(8, 361)
MgH <sub>2</sub>	STO-3G	(15, 2285)	(15, 289)	(15, 289)	(17, 3540)	(17, 3540)	(22, 4582)
CO	STO-3G	(12, 1599)	(12, 241)	(12, 241)	(16, 4409)	(16, 4409)	(20, 5475)
LiH	STO-3G	(4, 100)	(4, 35)	(4, 35)	(8, 558)	(8, 586)	(12, 631)
N <sub>2</sub>	STO-3G	(11, 815)	(11, 153)	(11, 153)	(15, 2229)	(15, 2229)	(20, 2975)
NaH	STO-3G	(14, 2722)	(14, 375)	(14, 375)	(16, 4409)	(16, 4409)	(20, 5851)
H <sub>2</sub> O	STO-3G	(7, 435)	(7, 73)	(7, 73)	(10, 1035)	(10, 1035)	(14, 1086)
H <sub>3</sub> <sup>+</sup>	STO-3G	(1, 3)	(1, 2)	(1, 2)	(3, 34)	(3, 35)	(6, 78)
LiOH	STO-3G	(13, 2104)	(13, 296)	(13, 296)	(18, 6852)	(18, 6852)	(22, 8758)
LiH	3-21G	(13, 2732)	(13, 375)	(13, 383)	(18, 6852)	(18, 6852)	(22, 8758)
H <sub>2</sub>	6-31G	(5, 122)	(5, 27)	(5, 27)	(5, 122)	(5, 124)	(8, 185)
NH <sub>4</sub> <sup>+</sup>	STO-3G	(12, 1359)	(12, 176)	(12, 176)	(14, 2194)	(14, 2194)	(18, 6892)
HF	STO-3G	(4, 100)	(4, 35)	(4, 35)	(8, 558)	(8, 558)	(12, 631)

TABLE VI: Different resource requirements to study different electronic structure Hamiltonians required to achieve chemical accuracy. Each round bracket tuple reports  $(n, |H|)$  and gives the number of qubits and terms for each Hamiltonian considered.  $RH_{\text{tapered}}R^\dagger$  describes the effect of the CS-VQE unitary partitioning rotation on the problem Hamiltonian and  $H_{\text{CS-VQE}} = Q_{\mathcal{W}}U_{\mathcal{W}}^\dagger H_{\text{full}}U_{\mathcal{W}}Q_{\mathcal{W}}^\dagger$ . The square tuple gives the upper bound of single qubit gates (SQG) and CNOT gates  $[SQG, CNOT]$  required to perform  $R$  as a sequence of rotations in the unitary partitioning measurement reduction step, based on the largest anticommuting clique - representing the largest possible circuit for  $R_S$ . The size of the Hamiltonian for LiH (3-21G singlet) with measurement reduction applied is different for the sequence of rotations and LCU unitary partitioning methods. This is an artifact of the graph colour heuristic finding different anticommuting cliques in the CS-VQE Hamiltonian.